Check for updates

Received: 6 November 2023 | Revised: 8 March 2024 | Accepted: 4 April 2024

DOI: 10.1002/ardp.202300634

FULL PAPER

ARCH PHARM DPhG
Archiv der Pharmazie

Synthesis and biological studies of pyrimidine derivatives targeting metabolic enzymes

Elif Korkusuz[1] | Yusuf Sert[2] | Seher Arslan[3] | Hava Aydın[3] | İsmail Yıldırım[3] | Yeliz Demir[4] | İlhami Gülçin[5] | İrfan Koca[6,7]

[1]Mustafa Cikrikcioglu Vocational College, Kayseri University, Kayseri, Turkey

[2]Department of Physics, Faculty of Art & Sciences, Yozgat Bozok University, Yozgat, Turkey

[3]Department of Chemistry, Erciyes University, Kayseri, Turkey

[4]Nihat Delibalta Gole Vocational High School, Ardahan University, Ardahan, Turkey

[5]Department of Chemistry, Faculty of Science, Atatürk University, Erzurum, Turkey

[6]Department of Chemistry, Faculty of Art & Sciences, Yozgat Bozok University, Yozgat, Turkey

[7]Science and Technology Application and Research Center, Yozgat Bozok University, Yozgat, Turkey

Correspondence
İrfan Koca, Department of Chemistry, Faculty of Art & Sciences, Yozgat Bozok University, Yozgat 66900, Turkey.
Email: i_koca@yahoo.com

Elif Korkusuz, Mustafa Cikrikcioglu Vocational College, Kayseri University, Kayseri 38039, Türkiye.
Email: elifkorkusuz@kayseri.edu.tr

Funding information
Scientific Research Projects Coordination Unit Coordinatorship of Erciyes University

Abstract

Novel synthesized pyrimidine derivatives were investigated against carbonic anhydrase isoenzymes I and II (hCA I and II), acetylcholinesterase (AChE), butyrylcholinesterase (BChE), α-glycosidase, and aldose reductase (AR) enzymes associated with some common diseases such as epilepsy, glaucoma, Alzheimer's disease, diabetes, and neuropathy. When the results were examined, novel synthesized pyrimidine derivatives were found to have effective inhibition abilities toward the metabolic enzymes. IC_{50} values and K_i values were calculated for each pyrimidine derivative and compared to positive controls. The synthesized novel pyrimidine derivatives exhibited K_i values in the range of 39.16 ± 7.70–144.62 ± 26.98 nM against hCA I, 18.21 ± 3.66–136.35 ± 21.48 nM toward hCA II, which is associated with different pathological and physiological processes, 33.15 ± 4.85–52.98 ± 19.86 nM on AChE, and 31.96 ± 8.24–69.57 ± 21.27 nM on BChE. Also, K_i values were determined in the range of 17.37 ± 1.11–253.88 ± 39.91 nM against α-glycosidase and 648.82 ± 53.74–1902.58 ± 98.90 nM toward AR enzymes. Within the scope of the study, the inhibition types of the novel synthesized pyrimidine derivatives were evaluated.

KEYWORDS
carbonic anhydrase, cholinesterase, enzyme inhibition, molecular docking, pyrimidine

1 | INTRODUCTION

Pyrimidine and its derivatives are common in nature and known to be used in a wide range of applications in pharmacologically active compounds. Pyrimidines and fused pyrimidines, being an integral part of DNA and RNA, play a vital role in a variety of biological activities.[1] Nucleosides of pyrimidine, such as cytarabine, floxuridine, and capecitabine, are indeed ratified with antitumor activity[2,3] (Figure 1). Pyrimidine derivatives are found to possess a wide range of pharmacological properties such as analgesic, antiarrhythmic, anti-inflammatory, antiparkinsonian, and androgenic–anabolic activities.[4,5] Various analogs of thiopyrimidones exhibited antibacterial, antifungal, antiviral, and antileishmanial activities.[6,7]

This is an open access article under the terms of the Creative Commons Attribution-NonCommercial-NoDerivs License, which permits use and distribution in any medium, provided the original work is properly cited, the use is non-commercial and no modifications or adaptations are made.
© 2024 The Authors. *Archiv der Pharmazie* published by Wiley-VCH GmbH on behalf of Deutsche Pharmazeutische Gesellschaft.

Thiadiazolopyrimidine derivatives are a class of fused heterocyclic compounds that have a wide range of biological activity and, as a result, have become a focus of interest for scientists. The thiadiazolo-pyrimidine nucleus and its substituted products, belonging to the pseudo purine class, had interesting biological profiles such as antiviral,[8] anticancer,[9] and antitubercular[10] activities. In the past few decades, these analogs were synthesized as PARP1 inhibitors and STAT3 inhibitors.[11,12] Also, [1,3,4]thiadiazolopyrimidine derivatives can be identified in the structure of different drugs; for example, compound **I** displays anthelmintic activity,[13] compound **II** is reported for fighting *Candida albicans* strain associated fungal infections,[14] and carbonic anhydrase (CA) inhibitors (compound **III**) and xanthine oxidase (XO) inhibitors (compound **IV**) are used for the treatment of glaucoma and gout, respectively[15–17] (Figure 2).

CA isoforms play a significant role in numerous physiological activities in eukaryotes, including electrolyte secretion, CO_2 transport, photosynthesis, and respiration, among others.[18–20] Mammals have been found to have 16 different CA isoforms, including CA I and CA II. These enzymes are members of the α-CA family. Furthermore, CA inhibitors (CAIs) have clinical applications in major diseases such as neurological disorders, gastroduodenal ulcers, glaucoma, diuretics, acid–base imbalances, and epilepsy, where they are used to determine their therapeutic roles.[21–23] Furthermore, it has been recently discovered that CAIs hold promise as potential treatments for obesity, epilepsy, infections, and cancer.[24–26] fhCA I is predominantly located at higher concentrations in the cytosol of erythrocytes.[27] In contrast, human carbonic anhydrase isoenzyme (hCA) II represents the most extensively studied isoform with regard to inhibitor design and structural aspects, making it a significant target in molecular dynamics simulations. Furthermore, it is the most widely distributed and physiologically relevant CA isoenzyme.[28,29] CA inhibitors have been shown to be beneficial and useful in the treatment of a variety of clinical conditions. Tolsultazolamide, ethoxzolamide, ethoxzolamide, diclofenamide, zonisamide, brinzolamide, and acetazolamide (AZA) are a few examples of these inhibitors. However, comprehensive examinations of these drugs' absorption, distribution, metabolism, and excretion in diverse organisms have been necessitated by their terrible adverse effects.[30] Therefore, new inhibitors need to be developed.

Alzheimer's disease (AD) exhibits a multifaceted phenotypic variation, deteriorating over time. It stands as the most common form of dementia among the elderly, marked by a decline in cognitive abilities encompassing attention, memory, orientation, language skills, and even the onset of depression.[31,32] In both vertebrates and insects, cholinesterases play a crucial role in hydrolyzing the neurotransmitter acetylcholine within the central and peripheral nervous systems.[33] Cholinesterases are responsible for transmitting nerve impulses to the cholinergic synapses throughout the body. Acetylcholinesterase (AChE) and butyrylcholinesterase (BChE) represent two distinct cholinesterase examples.[34] While AChE and BChE possess a comparable molecular structure, BChE exhibits a distinct preference for hydrolyzing acetyl esters, such as acetylcholine, compared to AChE. Another differentiating characteristic between AChE and BChE is the inhibition of AChE when there is an excess of the substrate. This property is linked to the catalytic process and the binding of the substrate.[35] Tacrine (TAC) is a pioneer of AChE/BChE inhibitors approved by the Food and Drug Administration (FDA) to treat AD. However, its clinical application has been restricted due to its poor therapeutic efficacy and high prevalence of detrimental effects.[36] Thus, it is very crucial to develop new AChE/BChE inhibitors.

Diabetes mellitus (DM) is a chronic metabolic disorder marked by elevated blood sugar levels (hyperglycemia) and disturbances in the metabolism of carbohydrates, lipids, and proteins.[37] The primary medical approach to managing the progression of DM and its associated complications revolves around lowering postprandial (after-meal) blood glucose levels.[38] This is achieved through the regulation and/or inhibition of carbohydrate-hydrolyzing enzymes. α-Glycosidases (Gly) play a crucial role in various biological processes that impact both health maintenance and the development of diseases.[39] Irregular glycosidase activities hold significant relevance in various health conditions, including lysosomal storage diseases, cancer, AD, viral infections, and diabetes.[40] For the treatment of these conditions, a number of glycosidase inhibitors, including voglibose, acarbose, miglitol, and miglustat, have been created. The

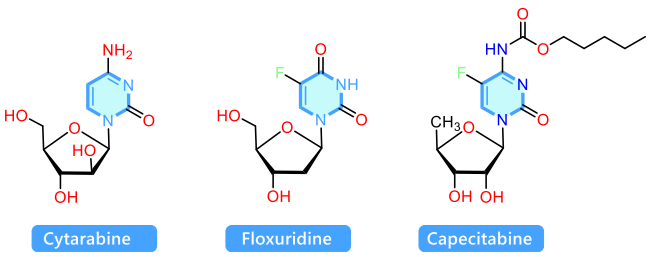


FIGURE 1 The structures of some nucleosides of pyrimidine derivatives.

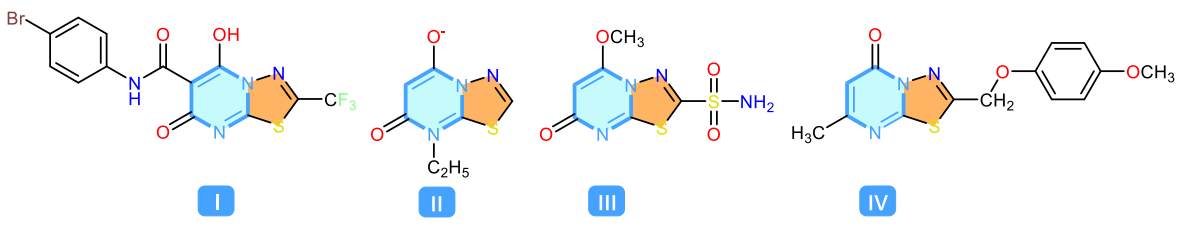


FIGURE 2 Some bioactive [1,3,4]thiadiazolopyrimidine derivatives.

15214184, 0, Downloaded from https://onlinelibrary.wiley.com/doi/10.1002/ardp.202300634 by BOZOK UNIVERSITY-YOZGAT, Wiley Online Library on [21/05/2024]. See the Terms and Conditions (https://onlinelibrary.wiley.com/terms-and-conditions) on Wiley Online Library for rules of use; OA articles are governed by the applicable Creative Commons License

usage of these inhibitors, however, may have unfavorable side effects, such as severe gastrointestinal problems like diarrhea and flatulence. Therefore, there is a pressing need for the creation of new inhibitors.[41,42]

As the first rate-limiting enzyme in the polyol pathway, aldose reductase (AR), an enzyme from the superfamily of aldo-keto reductases, aids in the conversion of glucose into sorbitol by using NADPH. Additionally, the sorbitol dehydrogenase enzyme is in charge of facilitating the conversion of sorbitol to fructose.[43] The polyol pathway typically contributes less than 3% of the total amount of glucose utilized and is regarded as a relatively small process for glucose metabolism. Although this route can account for up to 30% of total glucose utilization, it becomes more active as blood glucose levels rise. In people with diabetes, the aberrant activation of the polyol pathway causes an increase in sorbitol that is osmotically active, resulting in oxidative and osmotic stress that could harm tissue.[44] Inhibiting AR is thus a promising therapeutic research target because it provides a key strategy for avoiding and treating diabetes complications.[45] The only AR inhibitor that has received FDA approval and is now being used to treat diabetic neuropathy is epalrestat (EPR). Safety issues led to the withdrawal of several medications, while others are currently undergoing clinical trials.[46] Therefore, it is imperative to create novel AR inhibitors with enhanced safety and efficacy profiles.

The coupling of two or more biologically active heterocyclic rings, in either condensed or linked form, leads to a significant increase in the biological activity of such molecules. With this in mind, in this study, thiazolo pyrimidine and thiadiazolo pyrimidine derivatives were experimentally synthesized, and their inhibitory properties against some enzymes were investigated (Scheme 1). IR, NMR, and elemental analysis methods were employed for the identification of the newly synthesized chemicals. hCA I, hCA II, AChE, BChE, α-Gly, and AR were selected as target enzymes, and inhibition experiments were performed in comparison with appropriate standards. In the literature, there are separate studies on the effects of pyrimidine derivatives on the enzymes in this study; however, there is no existing study encompassing all five different enzymes together.[47–51] The reason for selecting these enzymes, each associated with distinct pathologies, is to better understand the biochemical mechanisms of these diseases and obtain crucial insights into potential multitargeted therapeutic strategies. Our primary focus is to identify and characterize inhibitors for these enzymes, aiming to develop a potential multitargeted therapeutic agent. Also, docking studies of the target compounds against each enzyme were performed.

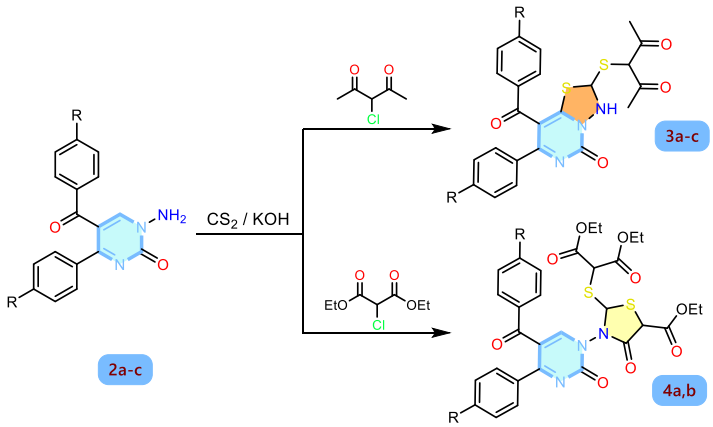
2 | RESULTS AND DISCUSSION

2.1 | Chemistry

N-Amino pyrimidine compounds (**2a–c**) used as starting materials were prepared from 2,3-furandione derivatives by a two-step synthesis process according to the literature.[52-54] The compounds **2a–c** in KOH medium with CS_2 were mixed in boiling acetonitrile to synthesize pyrimidine carbamodithioate (Scheme 1). Pyrimidine carbamodithioate derivatives were used freshly in the medium without isolation. Heating of pyrimidine carbamodithioate with 3-chloropentane-2,4-dione in acetonitrile afforded thiadiazolo[3,2-*c*]pyrimidine (**3**), which formed by loss of HCl molecule from the intermediate, followed by cyclization reaction. The chemical structures of **3a–c** were characterized by IR, ^{1}H NMR, ^{13}C NMR, and elemental analyses.

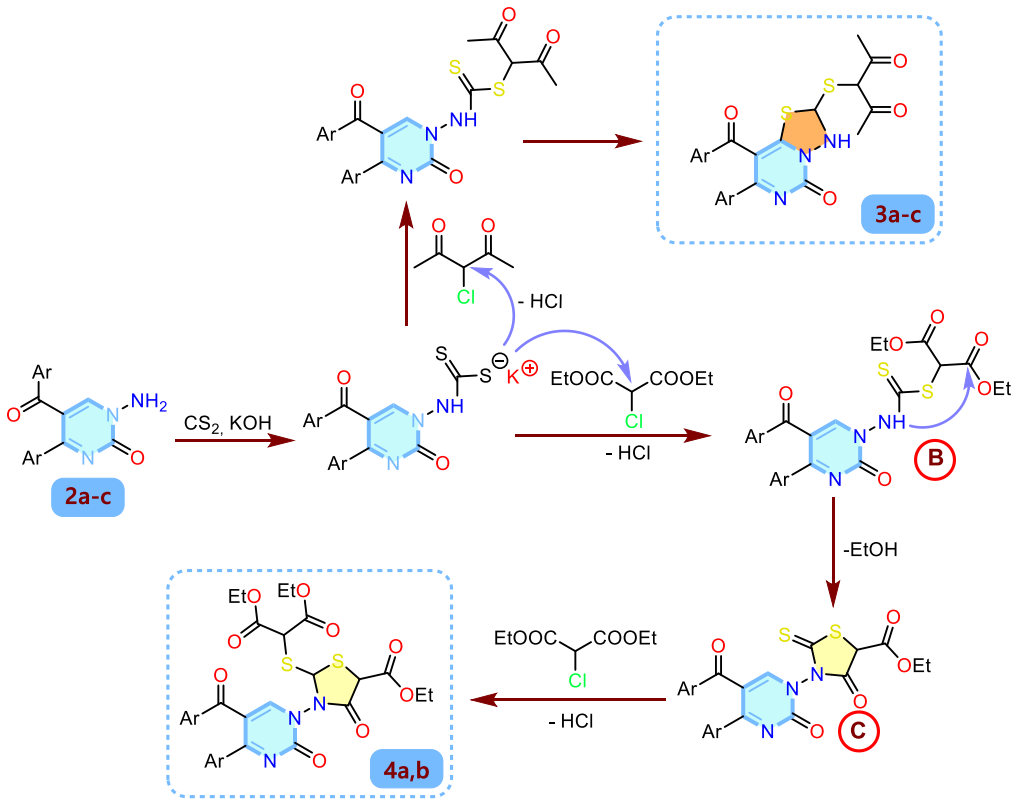
The absorptions of N–H and carbonyl functions were recorded in the IR spectrum at 3298, 1703, 1637, and 1614 cm^{-1}, respectively. In the ^{1}H NMR spectrum, the proton of NH of the thiadiazole ring was observed as a singlet at deshielded field, δ 10.32 ppm. Elemental analysis values, which confirmed the molecular formula $C_{23}H_{19}N_3O_4S_2$, were found to be in good agreement with the calculated values (±0.4%).

The thiazolyl-pyrimidine derivatives **4** were obtained using the same procedure as thiadiazolo[3,2-*c*]pyrimidine derivatives. The structure of **4** was elucidated from the results of the spectral analyses. The proposed mechanism for the reaction of pyrimidine carbamodithioates with diethyl chloro malonate involves the nucleophilic substitution of pyrimidine carbamodithioate through its –SK



SCHEME 1 The synthesis of target compounds.

15214184, 0, Downloaded from https://onlinelibrary.wiley.com/doi/10.1002/ardp.202300634 by BOZOK UNIVERSITY-YOZGAT, Wiley Online Library on [21/05/2024]. See the Terms and Conditions (https://onlinelibrary.wiley.com/terms-and-conditions) on Wiley Online Library for rules of use; OA articles are governed by the applicable Creative Commons License



SCHEME 2 Possible reaction mechanism of formation of target compounds.

group to the positive C-2 position of diethyl chloro malonate to yield the intermediate (**B**) (Scheme 2). The heterocyclization of the intermediate (**B**) was assumed to occur by the addition of –NH group to the carbonyl groups to produce the imino-perhydropyridine intermediate (**C**). The thiazol-pyrimidine derivatives **4** were formed by the nucleophilic attack of S group of intermediate (**C**) to second molecule diethyl chloro malonate, followed by loss of HCl. The ^{1}H NMR spectrum of **4a** showed two singlets at δ 5.56, 5.32 ppm for two protons corresponding to –CH groups. The aromatic protons were observed as multiplets at δ 7.39–6.97 ppm. The proton of $-CH_3$ groups resonates three triplets at δ 4.34–4.25 ppm. The ^{13}C NMR spectrum displayed 10 carbon signals corresponding to 26 carbon atoms.

2.2 | Inhibition studies

The influences of pyrimidine derivatives against hCAs, AChE, BChE, AR, and α-glycosidase were analyzed using an in vitro inhibition investigation. The obtained results (IC_{50} and K_i values) for all the synthesized target compounds (**2a–c, 3a–c, 4a**, and **4b**) and standard inhibitors (AZA, TAC, ACR, and EPR) are tabulated in Tables 1 and 2.

i-) All tested compounds displayed promising hCA I inhibitory potential with IC_{50} values in the range of 36.47–121.56 nM (Table 1). In the set of compounds (**3a–c**), the most active compound was **3a** (3-[(7-benzoyl-6-phenyl-4-oxo-2,3-dihydro-4*H*-[1,3,4]thiadiazolo[3,2-c]pyrimidine-2-yl)thio] pentane-2,4-dione) with a K_i value of 65.63 nM for hCA I (Figure 3). Disappointingly, adding 4-OCH_3 next to the benzoyl group (**3c**) moiety significantly lessened the inhibitory effect (about 1.55-fold). Replacement of 4-OCH_3 in **3c** with $4CH_3$ (**3b**) moiety increased inhibition value. When compounds **4a** and **4b** are compared, the binding of the OCH_3 group at the 4th position in addition to the benzoyl group caused a 2.14-fold decrease in the hCA I enzyme inhibition value. All the compounds, except **2a–c**, and **3c** were more effective than AZA (K_i: 98.65 ± 22.65 nM) for hCA I. The potency of **3a, 3b**, and **3c** indicated the following order for hCA II: **3a** (K_i: 47.76 ± 12.71 nM) > **3c** (K_i: 49.02 ± 1.20 nM) > **3b** (K_i: 122.34 ± 41.13 nM). Replacement of four –OCH_3 in **3c** with four –CH_3 (**3b**) moiety decreased inhibition value. Comparison of the 2-oxo-1(2H)-[4-ethylmethanoat-2-(diethylpropanoat-thio)-1,3-thiazol-5-one-1-yl]pyrimidine derivatives, addition to the methoxy group at the 4th position decreased inhibition value 3.93-fold. All the compounds, except **2a** and **3b** were more effective than AZA (K_i: 87.21 ± 45.66 nM) for hCA II isoform.

ii-) According to the results reported in Table 1, all compounds showed high potency against AChE with an IC_{50} value ranging from 21.00 to 53.31 nM. In the set of compounds (**2a–c**), the most active compound was **2c** with a K_i value of 50.36 nM for

15214184, 0, Downloaded from https://onlinelibrary.wiley.com/doi/10.1002/ardp.202300634 by BOZOK UNIVERSITY-YOZGAT, Wiley Online Library on [21/05/2024]. See the Terms and Conditions (https://onlinelibrary.wiley.com/terms-and-conditions) on Wiley Online Library for rules of use; OA articles are governed by the applicable Creative Commons License

TABLE 1 IC_{50} values of novel pyrimidine derivatives on hCAs, AChE, BChE, AR, and α-Gly enzymes.

Compounds	IC_{50} (nM) hCA I	r^2	hCA II	r^2	AChE	r^2	BChE	r^2	α-Gly	r^2	AR	r^2
2a	121.56	0.9856	115.78	0.9843	23.89	0.9748	54.67	0.9732	223.24	0.9867	852.56	0.9896
2b	110.43	0.9754	36.47	0.9715	15.21	0.9876	49.50	0.9756	69.30	0.9851	705.68	0.9878
2c	115.78	0.9745	27.86	0.9832	18.44	0.9877	43.31	0.9741	30.13	0.9869	546.98	0.9721
3a	63.00	0.9960	46.20	0.9954	21.00	0.9819	56.67	0.9812	86.63	0.9866	903.52	0.9978
3b	49.50	0.9836	57.75	0.9939	30.13	0.9786	63.00	0.9768	82.50	0.9848	716.65	0.9842
3c	69.30	0.9795	63.00	0.9818	49.50	0.9852	69.30	0.9789	99.00	0.9811	631.15	0.9969
4a	60.26	0.9706	43.31	0.9721	53.31	0.9785	69.30	0.9764	69.30	0.9804	762.38	0.9735
4b	36.47	0.9737	23.89	0.9941	46.20	0.9820	57.75	0.9962	30.13	0.9894	538.62	0.9845
AZA[a]	75.12	0.9878	82.50	0.9875	-	-	-	-	-	-	-	-
TAC[b]	-	-	-	-	63.31	0.9788	82.50	0.9813	-	-	-	-
ACR[c] [23]	-	-	-	-	-	-	-	-	118.00	0.9540	-	-
EPR[d]	-		-	-	-	-	-	-	-	-	296.34	0.9845

Abbreviations: AChE, acetylcholinesterase; AR, aldose reductase; BChE, butyrylcholinesterase; hCAs, human carbonic anhydrase isoenzymes.

[a]Acetazolamide (AZA) standard inhibitor for hCAs.

[b]Tacrine (TAC) standard inhibitor for AChE and BChE.

[c]Acarbose (ACR) standard inhibitor for α-glycosidase.

[d]Epalrestat (EPR) is standard inhibitor for AR.

TABLE 2 K_i values of novel pyrimidine derivatives on hCAs, AChE, BChE, AR, and α-glycosidase enzymes.

Compounds	K_i (nM) hCA I	hCA II	AChE	BChE	α-Gly	AR
2a	144.62 ± 26.98	136.35 ± 21.28	48.44 ± 4.21	61.10 ± 14.56	200.21 ± 40.46	1484.80 ± 125.44
2b	105.52 ± 26.21	70.52 ± 10.21	22.44 ± 8.65	57.44 ± 9.64	71.24 ± 35.66	1220.35 ± 137.88
2c	117.63 ± 29.78	63.64 ± 3.56	36.62 ± 9.44	50.36 ± 7.69	35.12 ± 9.75	752.56 ± 97.21
3a	65.63 ± 15.22	47.76 ± 12.71	33.15 ± 4.85	31.96 ± 8.24	38.41 ± 3.44	1902.58 ± 98.90
3b	90.51 ± 30.31	122.34 ± 41.13	45.79 ± 15.62	41.06 ± 5.83	111.67 ± 43.21	1281.24 ± 350.66
3c	101.55 ± 32.26	49.02 ± 1.20	43.49 ± 5.68	63.41 ± 18.24	79.24 ± 8.94	1229.23 ± 14.15
4a	39.16 ± 7.70	18.21 ± 3.66	35.69 ± 3.45	69.57 ± 21.27	253.88 ± 39.91	1600.12 ± 392.88
4b	83.91 ± 4.84	71.54 ± 20.36	52.98 ± 19.86	40.71 ± 8.04	17.37 ± 1.11	648.82 ± 53.74
AZA[a]	98.65 ± 22.65	87.21 ± 45.66	-	-	-	-
TAC[b]	-	-	58.21 ± 11.13	72.44 ± 25.68	-	-
ACR[c] [23]					132.74 ± 14.76	-
EPR[d]	-	-	-	-	-	877.21 ± 21.56

Abbreviations: AChE, acetylcholinesterase; AR, aldose reductase; BChE, butyrylcholinesterase; hCAs, human carbonic anhydrase isoenzymes.

[a]Acetazolamide (AZA) is standard inhibitor for hCAs.

[b]Tacrine (TAC) is standard inhibitor for AChE and BChE.

[c]Acarbose (ACR) is standard inhibitor for α-glycosidase.

[d]Epalrestat (EPR) is standard inhibitor for AR.

AChE. From the screening data of **3b** and **3c**, it was revealed that **3c** having 4-OCH_3 moiety showed a better inhibition effect compared to **3b** for AChE. **3a**, bearing a 7-benzoyl-6-phenyl skeletal framework, showed the best inhibition effect among others (**3a**, K_i: 33.15 ± 4.85 nM) (Figure 3). When compounds **4a** and **4b** were compared, the compound (**4b**) carrying the methoxy group showed less inhibition effect for AChE. Similar to the AChE enzyme, among compounds **3a, 3b**, and **3c**, compound **3a**

15214184, 0, Downloaded from https://onlinelibrary.wiley.com/doi/10.1002/ardp.202300634 by BOZOK UNIVERSITY-YOZGAT, Wiley Online Library on [21/05/2024]. See the Terms and Conditions (https://onlinelibrary.wiley.com/terms-and-conditions) on Wiley Online Library for rules of use; OA articles are governed by the applicable Creative Commons License

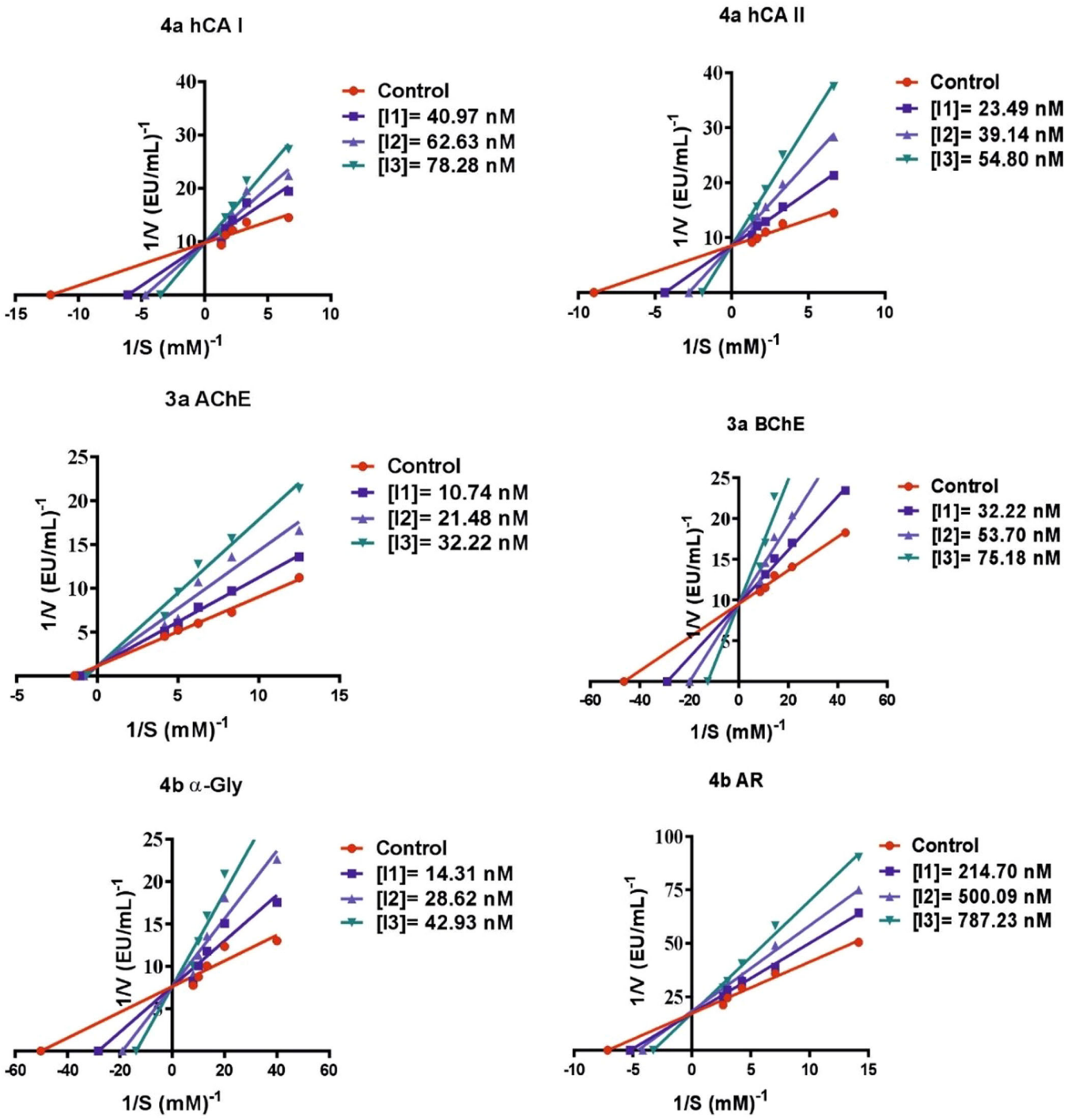


FIGURE 3 The Lineweaver–Burk plots of the best inhibitors for human carbonic anhydrase isoenzymes (hCAs), acetylcholinesterase (AChE), butyrylcholinesterase (BChE), aldose reductase (AR), and α-glycosidase enzymes.

(K_i: 31.96 ± 8.24 nM) showed the best inhibition value in the BChE enzyme. The potency of **3a, 3b**, and **3c** indicated the following order for BChE **3a** (K_i: 31.96 ± 8.24 nM, Figure 3) > **3b** (K_i: 41.06 ± 5.83 nM) > **3c** (K_i: 63.41 ± 18.24 nM). Unlike the AChE enzyme, the methoxy group was not effective in the BChE enzyme. Contrary to the AChE enzyme, when compounds **4a** and **4b** were compared, the compound (**4b**) bearing the methoxy group showed a better inhibition effect of BChE. All compounds studied for both AChE and BChE enzymes showed better inhibition effects than the standard inhibitor TAC (for AChE TAC, K_i: 58.21 ± 11.13 nM; for BChE TAC, K_i: 72.44 ± 25.68 nM).

iii-) The potency of **2a, 2b**, and **2c** indicated the following order for α-glycosidase: **2c** (K_i: 35.12 ± 9.75 nM) > **2b** (K_i: 71.24 ± 35.66 nM) > **2a** (K_i: 200.21 ± 40.46 nM). The potency

15214184, 0, Downloaded from https://onlinelibrary.wiley.com/doi/10.1002/ardp.202300634 by BOZOK UNIVERSITY-YOZGAT, Wiley Online Library on [21/05/2024]. See the Terms and Conditions (https://onlinelibrary.wiley.com/terms-and-conditions) on Wiley Online Library for rules of use; OA articles are governed by the applicable Creative Commons License

of **3a, 3b**, and **3c** indicated the following order for α-glycosidase: **3a** (K_i: 38.41 ± 3.44 nM) > **3c** (K_i: 79.24 ± 8.94 nM) > **3b** (K_i: 111.67 ± 43.21 nM). When compounds **4a** and **4b** are compared, the binding of the OCH_3 group at the 4th position in addition to the methoxy group caused a 14.62-fold decrease in the α-glycosidase enzyme inhibition value. In the 3-coded compounds, binding of the methoxy group instead of the methyl group caused an increase in the enzyme inhibition value. All tested compounds displayed promising AR inhibitory potential with IC_{50} values in the range of 538.62–903.52 nM (Table 1). The potency of **2a, 2b**, and **2c** indicated the following order for AR: **2c** (K_i: 752.56 ± 97.21 nM) > **2b** (K_i: 1220.35 ± 137.88 nM) > **2a** (K_i: 1484.80 ± 125.44 nM). In the set of compounds (**3a–c**), the most active compound was **3c** with a K_i value of 1229.23 nM for AR. Replacement of 4-OCH_3 in **3c** with 4-CH_3 (**3b**) moiety increased inhibition value. When compounds **4a** and **4b** were compared, the compound (**4b**, Figure 3) bearing the methoxy group showed a better inhibition effect of AR (**4a**, K_i: 1600.12 ± 392.88 nM; **4b**, K_i: 648.82 ± 53.74 nM). All inhibitors except **2c** and **4b** showed less inhibition effect than EPR (877.21 ± 21.56 nM).

2.3 | Molecular docking analysis

Molecular docking is a critical computational tool for drug design as it allows researchers to predict the binding affinity and mode of interaction between a small molecule drug candidate and its protein target, providing valuable insights for optimizing drug efficacy and reducing potential side effects. Additionally, this method involves the use of sophisticated algorithms and computational models to simulate the binding process between the drug molecule and its target protein, taking into account factors such as electrostatics, van der Waals forces, hydrogen bonding, and steric hindrance. By analyzing the binding energy and the key residues involved in the drug–target interaction, researchers can optimize the drug candidate's chemical structure and improve its binding affinity and selectivity for the target protein. This can help accelerate the drug discovery process and reduce the cost and risk associated with traditional trial-and-error methods.[55-57] There is quite a bit of theoretical work done in this area; so in this part of our study, we used molecular docking to examine the interactions between molecules and selected targets. The title compounds' and tested molecules' (AZA, TAC, and EPR) in silico molecular docking interactions with the hCAI-II, BChE, α-Gly, and AR receptors were examined using the AutoDock Vina program.[55] We will review the steps in this section. The ligands were first optimized in the gas phase using the Gaussian 09 W package program[58] using the Density Functional Theory (DFT) method/B3LYP functional and 6-311++G (d, p) basis set. As a result, the optimized ligands were depicted as in Figure 4 by using Gauss View 5.0 interface program[57] (based on their Gaussian 09 W numbering system). At the end of the Gaussian 09W calculation, the sum of electronic and zero-point energy values of the optimized structures (**2a–c**, **3a–c**, **4a,b**) was computed as −2770.06807892 a.u, −2996.57838287 a.u, −2128.39530853 a.u, −2206.03896295 a.u, −2354.90519977 a.u, −964.95733755 a.u, −1043.16700218 a.u, and −1192.75239213 a.u, respectively. The **4b** molecule is the most stable structure, according to the calculated DFT energy values.

Then, the ligands' pdb forms were recorded. Using the software Discover Studio Visualizer 4.0 (DSV 4.0),[59] each structure was later

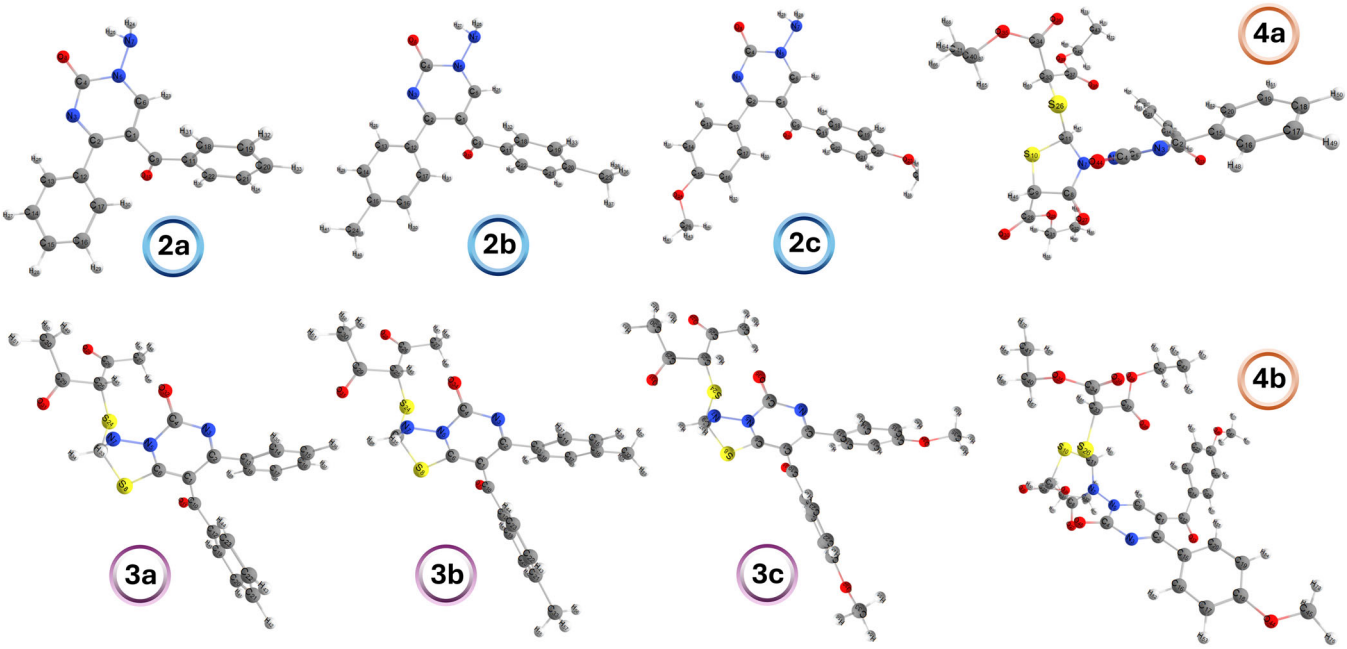


FIGURE 4 The optimized structures of studied molecules.

15214184, 0, Downloaded from https://onlinelibrary.wiley.com/doi/10.1002/ardp.202300634 by BOZOK UNIVERSITY-YOZGAT, Wiley Online Library on [21/05/2024]. See the Terms and Conditions (https://onlinelibrary.wiley.com/terms-and-conditions) on Wiley Online Library for rules of use; OA articles are governed by the applicable Creative Commons License

stored in pdb and pdbqt forms in accordance with their torsional angles. In the next step, the target proteins were chosen as hCAI/PDB: 2CAB,[60,61] hCAII/PDB: 5AML,[61,62] AChE/PDB: 1EVE,[61,63] BChE (PDB: 5NN0),[64,65] α–Gly (PDB: 1R47-A and -B chains),[65,66] and AR (PDB: 3V36)[67,68] according to experimental process and literature and 3D-pdb versions of the receptors were downloaded from RCSB (Protein Data Bank).[69] Using the software Discover Studio Visualizer 4.0 (DSV 4.0), the hetero atoms in the six targets were eliminated, the polar hydrogen charges were added, and the data were again recorded in pdb format.[69] The active sites/residues of the proteins were determined as follows to make the docking technique more efficient: HIS119, HIS96, and HIS94 for hCAI/PDB: 2CAB; THR200, THR199, LEU198, PHE131, VAL121, HIS119, HIS96, HIS94, GLN92, ASN67, and ASN62 for hCAII/PDB: 5AML; HIS440, PHE330, GLU327, TRP279, SER200, and TRP84 for AChE/PDB: 1EVE; ASN272, GLU271, ARG268, THR265, VAL264, SER263, LYS262, PRO261, ILE260, ALA245, LEU228, ASP216, PRO215, SER214, GLY213, LEU212, PRO211, SER210, TYR209, GLN183, ASN160, SER159, TRP111, HIS110, TY48, ASP43, LYS21, PRO20, THR19, and GLY18 for AR (PDB: 3V36). The grid parameters were established based on the co-factor molecules found in the 5NN0 and 1R47 proteins because the active sites of those proteins could not be identified from the literature or from their 3-D structures. In this way, the grid parameters were selected as $40 \times 40 \times 40$ Å^3 *x,y,z* dimensions, 0.375 Å space, and 39.041, −10.534, 10.394 *x,y,z* centers for hCAI/PDB: 2CAB; $32 \times 40 \times 32$ Å^3 *x,y,z* dimensions, 0.375 Å space, and −5.915, 5.359, 16.391 *x,y,z* centers for hCAII/PDB: 5AML; $44 \times 44 \times 38$ Å^3 *x,y,z* dimensions, 0.375 Å space, and −0.39, 63.448, 67.71 *x,y,z* centers for AChE/PDB: 1EVE; $40 \times 48 \times 40$ Å^3 *x,y,z* dimensions, 0.375 Å space, and 16.162, 39.021, 41.281 *x,y,z* centers for BChE/PDB: 5NN0; $40 \times 40 \times 40$ Å^3 *x,y,z* dimensions, 0.375 Å space, and 2.132, 56.598, 94.4 *x,y,z* centers for α-Gly/PDB: 1R47 (A and B chains), and $50 \times 40 \times 40$ Å^3 *x,y,z* dimensions, 0.375 Å space, and 2.842, 6.885, 22.574 *x,y,z* centers for AR (PDB: 3V36). According to the binding energy values, the final molecular docking scores are shown in Table 3 as kcal/mol. For **4a**+2CAB, **4a**+5AML, **3a**+1EVE, **3a**+5NN0, **4b**+1R47, **4b**+3V36, AZA+2CAB, AZA+5AML, TAC+1EVE, TAC+5NN0, Epalrestat+3V36, and Acarbose+1R47, docking shapes and their bond lengths are depicted as the positions of the ligands in the protein (a), 3D (b), and 2D (c) in Figures 5–16, respectively. As seen in Table 3, molecular docking calculations were made with four currently used drugs, namely AZA,[70] TAC,[71] EPR,[46] and ACR,[23] to compare the interactions.

The other interactions are depicted in Supporting Information S1: Figures S1–S42). Now, if we look at each interaction separately: When the findings were analyzed from Table 3, it was shown that the **4a** could inhibit the hCAI/PDB: 2CAB with −10.1 kcal/mol, **4a** could inhibit the hCAII/PDB: 5AML with −10.6 kcal/mol, **3a** could inhibit the AChE/PDB: 1EVE with −10.2 kcal/mol, **3a** could inhibit the BChE/PDB: 5NN0 with −10.2 kcal/mol, **4b** could inhibit the α-Gly/PDB: 1R47 with −10.6 kcal/mol, and finally, **4b** could inhibit the AR-PDB: 3V36 with −8.4 kcal/mol energies (to be highly potent inhibitor according to binding energy). In other words, it was seen that the best bindings occurred in **4a** (for 2CAB and 5AML), **3a** (for 1EVE and 5NN0), and **4b** (for 1R47 and 3V36) molecules.

Now, if we evaluate the obtained results in Table 3 in order: first, when the ligands (**2a–c**, **3a–c**, **4a**, **4b**)+hCAI/PDB:2CAB interactions were evaluated in terms of energy, the following ranking was found: **4a > 3a > 4b > 3b > 3c = 2b > 2c > 2a**. Second, the energy rankings for the interactions with the ligands (**2a–c, 3a–c, 4a,b**)+hCAII/PDB:5AML were as follows: **4a > 3a > 3c = 2c > 2b > 4b > 3b = 2a**. Third, the following ranking was discovered when the ligands (**2a–c**, **3a–c**, **4a,b**)+AChE/PDB:1EVE interactions were assessed in terms of energy: **3a > 4a = 2b = 2c > 3b = 3c > 4b = 2a**. Fourth, the following ranking was discovered when the interactions between the ligands (**2a–c**, **3a–c**, **4a**, **4b**)+BChE/PDB:5NN0 were assessed in terms of energy: **3a > 4b = 3b > 2c > 3c = 2a = 2b > 4a**. Fifth, when the ligands (**2a–c**, **3a–c**, **4a**, **4b**)+α-Gly/PDB:1R47 interactions were evaluated in terms of energy, the following ranking was found: **4b > 2c > 3a > 2b > 3c > 3b > 2a > 4a**. The ligands (**2a–c**, **3a–c**, **4a**, **4b**)+AR-/PDB:3V36 interactions were ranked according to their energy in the final section, and the results were as follows: **4b > 2c > 2b > 2a = 3b = 3c > 4a > 3a**. The final step was to compute and report the K_i values of the docking interactions in Table 3 using the equation $K_i = \exp(-G/RT)$, where *G* stands for binding energy, *R* stands for gas constant, which is equal to 1.987203610^{-3} kcal/mol, and *T* stands for room temperature, which is equal to 298.15 K. It is interesting that the **4a**, **3a**, and **4b** compounds have a very high potential to inhibit the relevant proteins and are highly consistent with the experimental results when all the results are combined.

3 | CONCLUSION

A novel series of pyrimidine derivatives were rationally designed, synthesized, and evaluated for their hCAs, AChE, BChE, AR, and α-glycosidase enzymes inhibitory effect. All tested derivatives demonstrated better hCAs, AChE, BChE, AR, and α-glycosidase inhibitory potential. Then, some structure–activity relationships were discussed in detail and molecular docking properties were performed to increase the understanding of the effect of the target compounds on the mentioned metabolic enzymes. These results indicate that the present compounds may have a positive potential as inhibitors of hCA I, hCA II, AChE, BChE, AR, α-glycosidase, and BChE, especially for epilepsy, glaucoma, AD, diabetes, and neuropathy, which are widely found worldwide.

4 | EXPERIMENTAL

4.1 | Chemistry

4.1.1 | General

Reagents and solvents were purchased from Merck, Fluka, and Sigma and used without further purification. For purity tests,

15214184, 0, Downloaded from https://onlinelibrary.wiley.com/doi/10.1002/ardp.202300634 by BOZOK UNIVERSITY-YOZGAT, Wiley Online Library on [21/05/2024]. See the Terms and Conditions (https://onlinelibrary.wiley.com/terms-and-conditions) on Wiley Online Library for rules of use; OA articles are governed by the applicable Creative Commons License

TABLE 3 Molecular docking scores of title compounds and reference chemicals.

Compounds	hCA I/PDB: 2CAB Binding energy (kcal/mol)	N.H.B	K_i values (nM)	hCA II/PDB: 5AML Binding energy (kcal/mol)	N.H.B	K_i values (nM)	AChE/PDB: 1EVE Binding energy (kcal/mol)	N.H.B	K_i values (nM)
2a	−9.3	4	152.423	−9.4	0	128.751	−9.9	4	55.3665
2b	−9.5	3	108.755	−9.8	3	65.5462	−10.1	1	39.5045
2c	−9.4	4	128.755	−9.9	2	55.3665	−10.1	1	39.5045
3a	−9.8	2	65.5462	−10.0	4	46.7678	−10.2	2	33.3692
3b	−9.6	2	91.8647	−9.4	3	128.751	−10.0	2	46.7678
3c	−9.5	1	108.755	−9.9	2	55.3665	−10.0	2	46.7678
4a	−10.1	3	39.5045	−10.6	7	16.988	−10.1	2	39.5045
4b	−9.7	3	77.5976	−9.7	7	77.5976	−9.9	2	55.3665
AZA	−9.6	2	91.8647	−9.7	5	77.5976	-	-	-
TAC	-	-	-	-	-	-	−9.9	1	55.3665
Epalrestat	-	-	-	-	-	-	-	-	-
ACR	-	-	-	-	-	-	-	-	-
	BChE/PDB:5NN0 Binding energy (kcal/mol)	N.H.B	K_i values (nM)	**α-Gly/PDB:1R47** Binding energy (kcal/mol)	N.H.B	K_i values (nM)	**AR/PDB:3V36** Binding energy (kcal/mol)	N.H.B	K_i values (nM)
2a	−9.8	3	65.5462	−9.2	5	180.448	−8.0	2	1367.59
2b	−9.8	2	65.5462	−9.8	3	65.5462	−8.1	2	1155.2
2c	−9.9	4	55.3665	−10.2	5	33.3692	−8.3	2	824.244
3a	−10.2	1	33.3692	−10.1	6	39.5045	−7.8	2	1916.72
3b	−10.1	0	39.5045	−9.5	5	108.755	−8.0	2	1367.59
3c	−9.8	1	65.5462	−9.7	5	77.5976	−8.0	3	1367.59
4a	−9.7	1	77.5976	−9.0	5	252.902	−7.9	3	1619.04
4b	−10.1	1	39.5045	−10.6	6	16.958	−8.4	3	696.234
AZA	-	-	-	-	-	-	-	-	-
TAC	−9.7	1	77.5976	-	-	-	-	-	-
Epalrestat	-	-	-	-	-	-	−8.3	3	824.244
ACR	-	-	-	−9.4	7	128.751	-	-	-

Abbreviations: AChE, acetylcholinesterase; ACR, acarbose; AR, aldose reductase; AZA, acetazolamide; BChE, butyrylcholinesterase; EPR, epalrestat; hCAs, human carbonic anhydrase isoenzymes; TAC, tacrine.

TLC: Merck precoated silica gel plates 60F 254. Mp.: Electrothermal 9200 apparatus; uncorrected. IR Spectra: Shimadzu 8400 FT-IR spectrometer; in cm^{-1}. ^1H- and ^{13}C NMR Spectra: Bruker Avance III Ultrashield spectrometer operating at 400.13 MHz (^1H) and 100.61 MHz (^{13}C) in (D6) DMSO and/or $CDCl_3$; δ in ppm, coupling constants J in Hz. The following abbreviations are used: singlet (s), doubled (d), triplet (t), doubled triplet (dt), doubled doubled (dd), multiplet (m), broad signal (br). When necessary to identify all carbon atoms, complementary NMR experiments (COSY and APT) were performed. Elemental analyses (C, H, N, S): LECO-932 CHNS-O analyzer.

4.1.2 | General procedure for the preparation of the target compounds

To the solution of *N*-amino pyrimidine compounds (**2a–c**, 1 mmol) in approximately 20 mL of acetonitrile was added 0.06 g KOH (1 mmol) of water solution (10 mL). After stirring for 5 min, 0.18 mL of CS_2 (3 mmol) was added dropwise. The reaction flask was heated at reflux conditions and stirred for approximately 20 min. Then, the heating process was stopped and cooled to room temperature. Then, 4 mmol of 3-chloropentane-2,4-dione (for **3a–c**) or diethyl 2-chloromalonate (for **4a**,**b**) was added

15214184, 0, Downloaded from https://onlinelibrary.wiley.com/doi/10.1002/ardp.202300634 by BOZOK UNIVERSITY-YOZGAT, Wiley Online Library on [21/05/2024]. See the Terms and Conditions (https://onlinelibrary.wiley.com/terms-and-conditions) on Wiley Online Library for rules of use; OA articles are governed by the applicable Creative Commons License

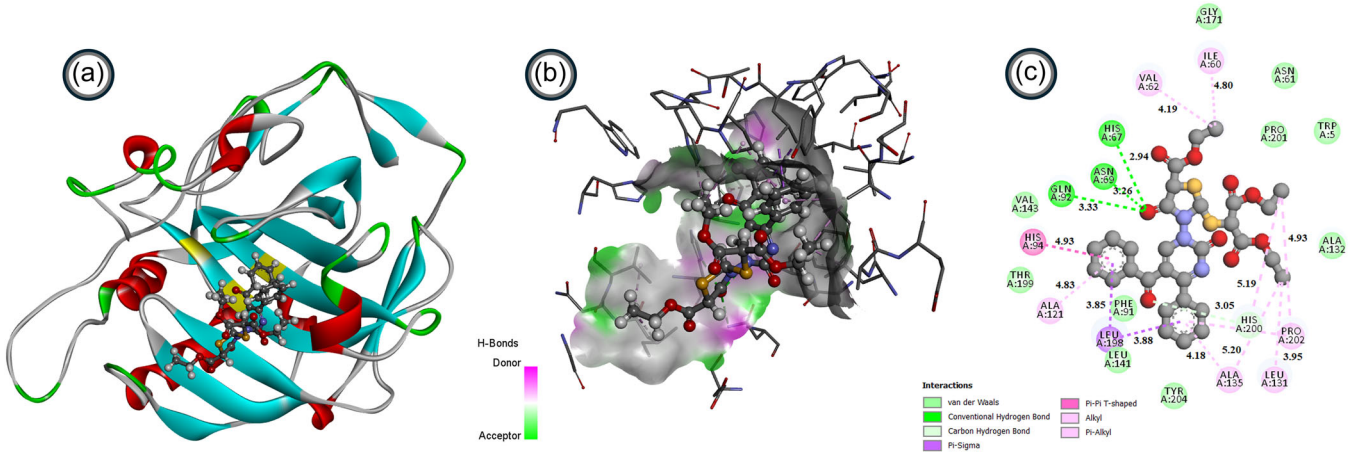


FIGURE 5 The position of the **4a** ligand in the PDB: 2CAB protein (a), 3D (b), and 2D (c) molecular docking results.

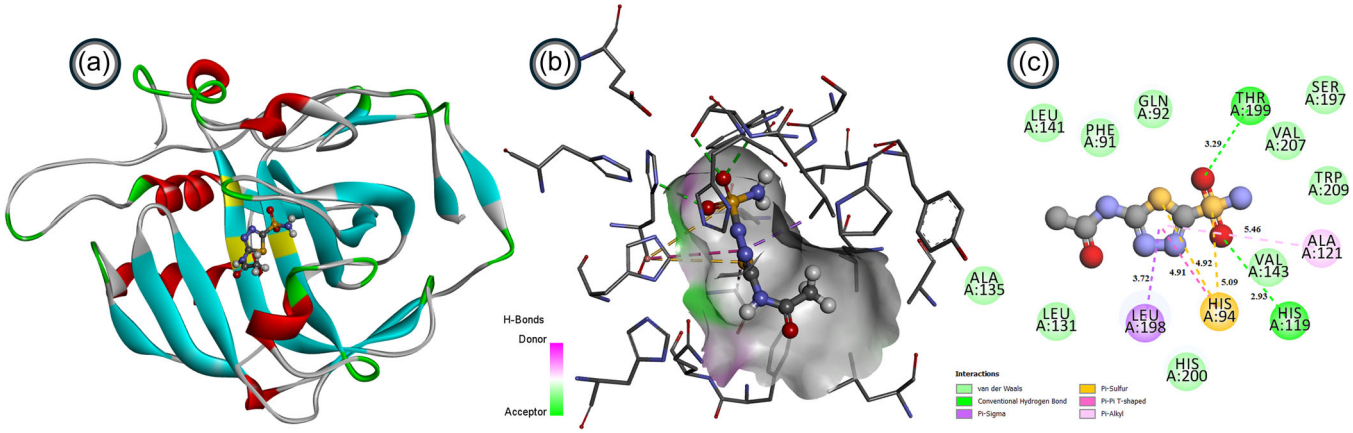


FIGURE 6 The position of the acetazolamide ligand in the PDB: 2CAB protein (a), 3D (b), and 2D (c) molecular docking results.

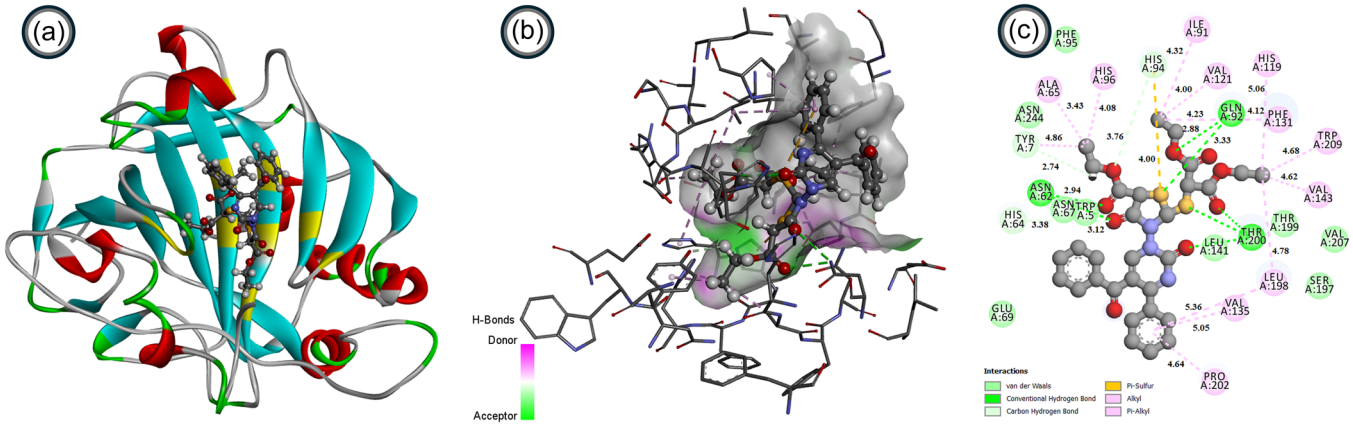


FIGURE 7 The position of the **4a** ligand in the PDB: 5AML protein (a), 3D (b), and 2D (c) molecular docking results.

dropwise to the reaction flask. It was placed in a reflux cooler and boiled for 7–15 h. At the end of the time, the reaction vessel was cooled to room temperature and approximately 50 mL of ice water was added to it and stirred for 2–3 h. Diethyl ether was added, and extraction was carried out. Petroleum ether was added to the separated organic phase, and the crude product was precipitated and filtered. The crude product formed was recrystallized from a suitable solvent.

15214184, 0, Downloaded from https://onlinelibrary.wiley.com/doi/10.1002/ardp.202300634 by BOZOK UNIVERSITY-YOZGAT, Wiley Online Library on [21/05/2024]. See the Terms and Conditions (https://onlinelibrary.wiley.com/terms-and-conditions) on Wiley Online Library for rules of use; OA articles are governed by the applicable Creative Commons License

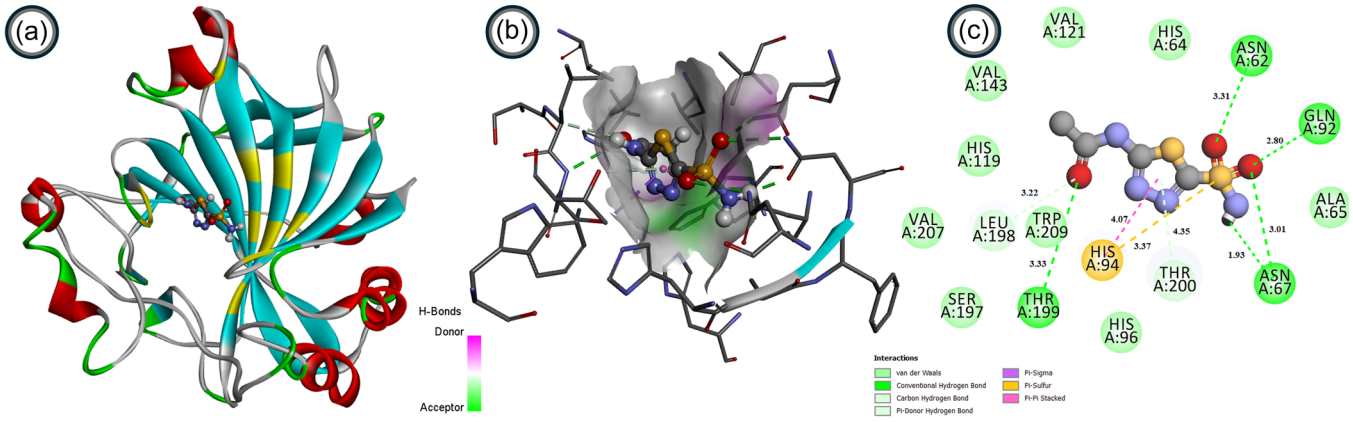


FIGURE 8 The position of the tacrine ligand in the PDB: 5AML protein (a), 3D (b), and 2D (c) molecular docking results.

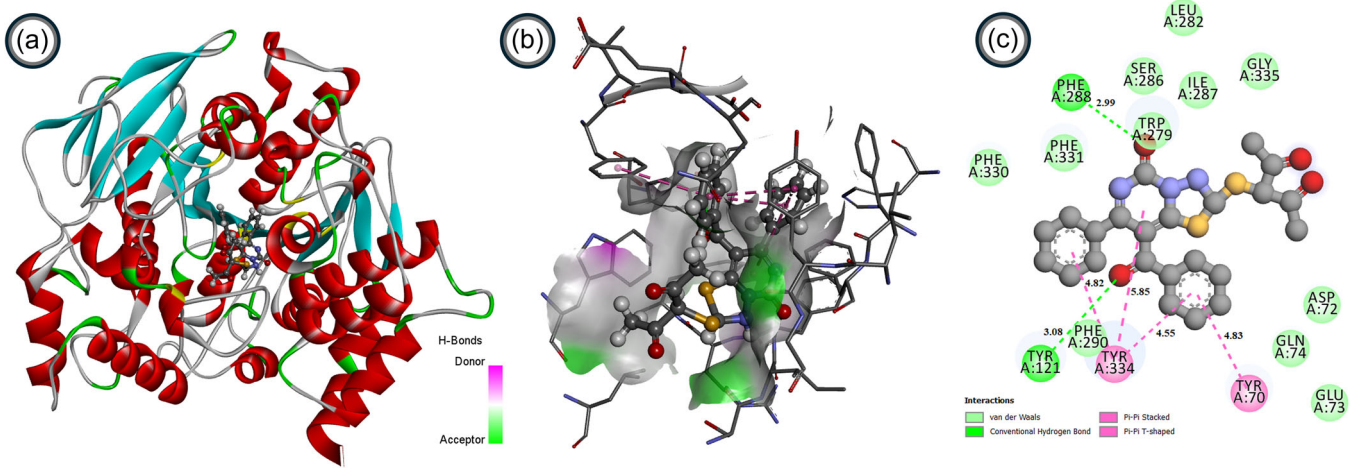


FIGURE 9 The position of the **3a** ligand in the PDB: 1EVE protein (a), 3D (b), and 2D (c) molecular docking results.

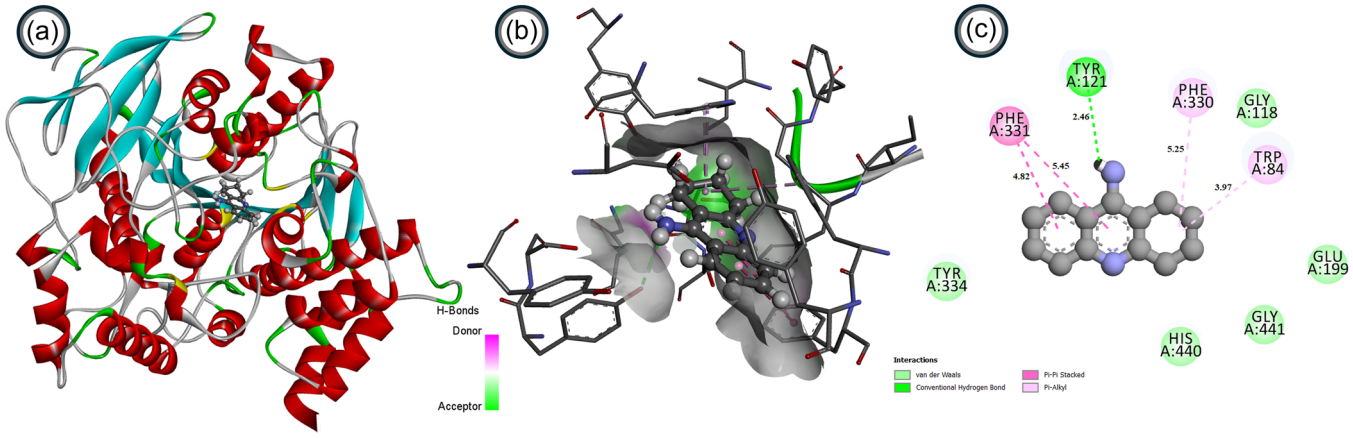


FIGURE 10 The position of the tacrine ligand in the PDB: 1EVE protein (a), 3D (b), and 2D (c) molecular docking results.

15214184, 0, Downloaded from https://onlinelibrary.wiley.com/doi/10.1002/ardp.202300634 by BOZOK UNIVERSITY-YOZGAT, Wiley Online Library on [21/05/2024]. See the Terms and Conditions (https://onlinelibrary.wiley.com/terms-and-conditions) on Wiley Online Library for rules of use; OA articles are governed by the applicable Creative Commons License

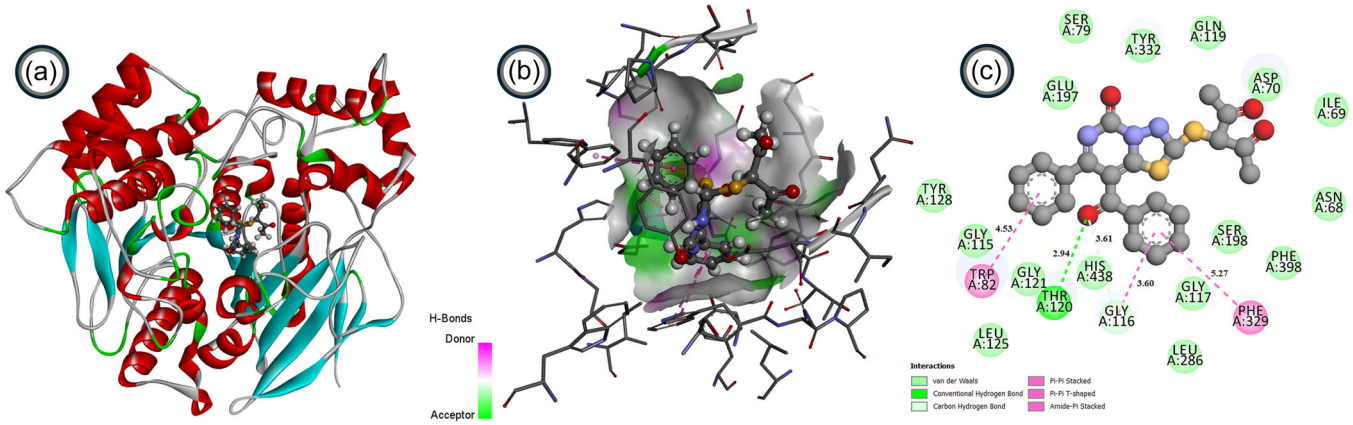


FIGURE 11 The position of the **3a** ligand in the PDB: 5NN0 protein (a), 3D (b), and 2D (c) molecular docking results.

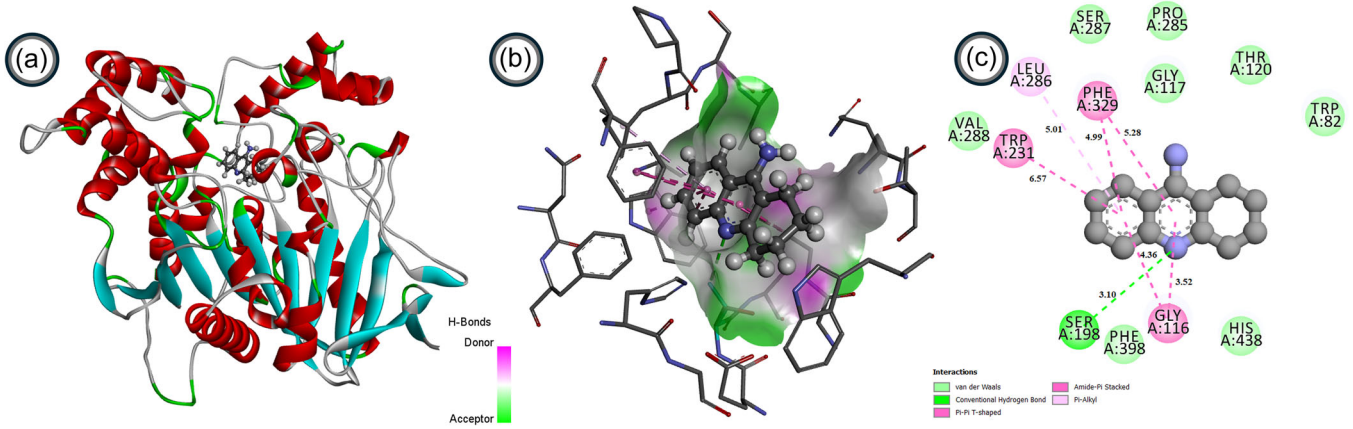


FIGURE 12 The position of the tacrine ligand in the PDB: 5NN0 protein (a), 3D (b), and 2D (c) molecular docking results.

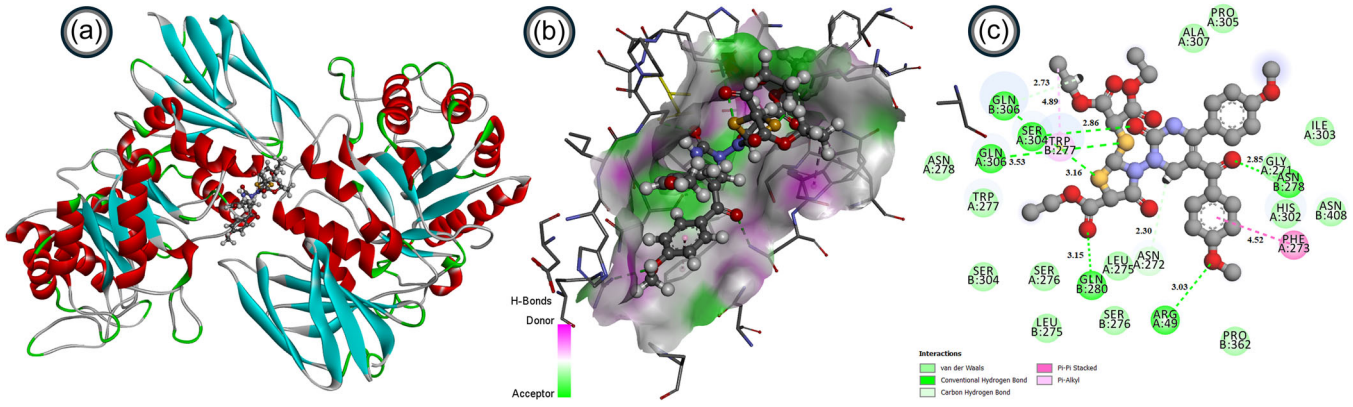


FIGURE 13 The position of the **4b** ligand in the PDB: 1R47 protein (a), 3D (b), and 2D (c) molecular docking results.

15214184, 0, Downloaded from https://onlinelibrary.wiley.com/doi/10.1002/ardp.202300634 by BOZOK UNIVERSITY-YOZGAT, Wiley Online Library on [21/05/2024]. See the Terms and Conditions (https://onlinelibrary.wiley.com/terms-and-conditions) on Wiley Online Library for rules of use; OA articles are governed by the applicable Creative Commons License

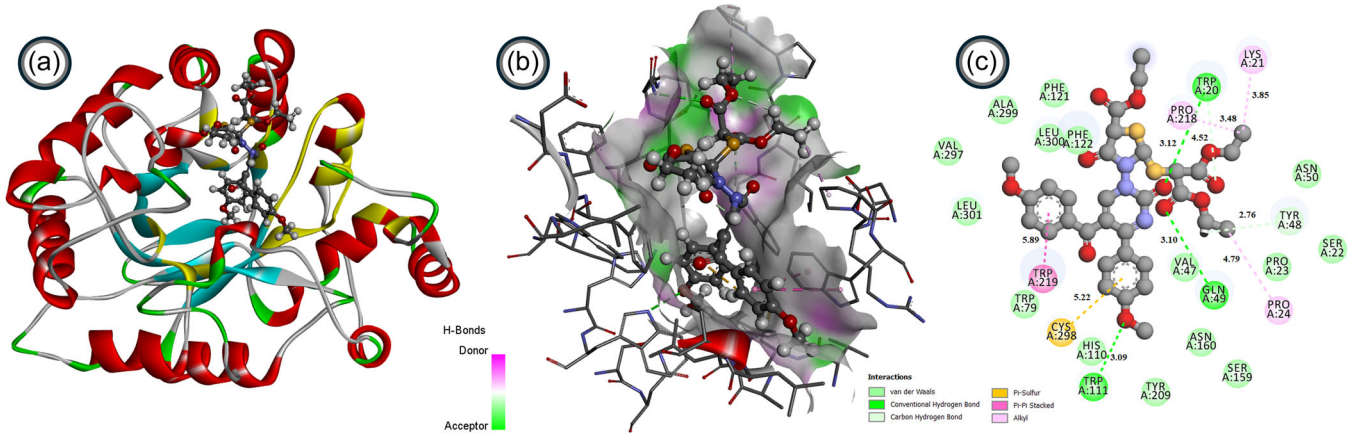


FIGURE 14 The position of the **4b** ligand in the PDB: 3V36 protein (a), 3D (b), and 2D (c) molecular docking results.

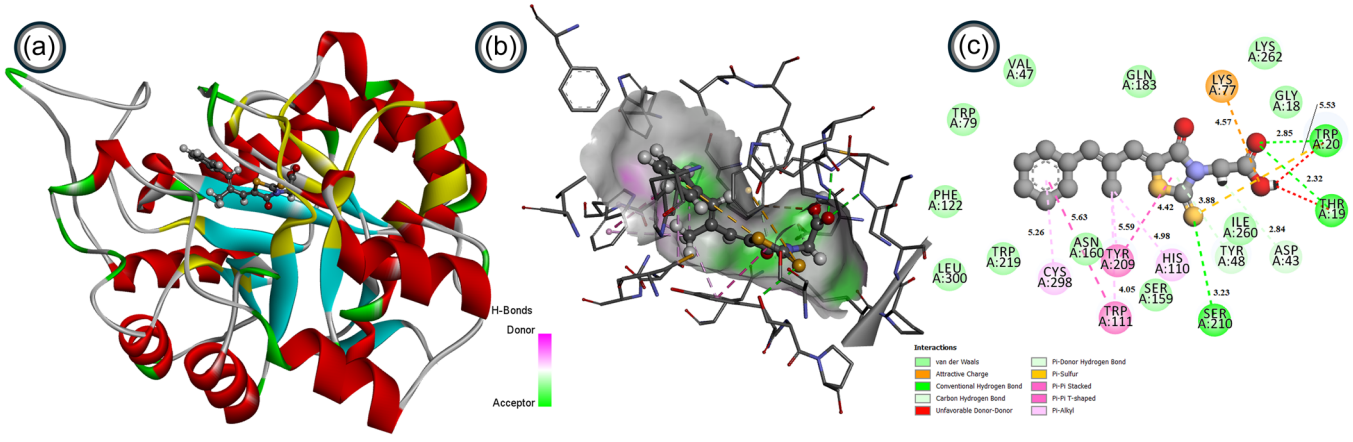


FIGURE 15 The position of the epalrestat ligand in the PDB: 3V36 protein (a), 3D (b), and 2D (c) molecular docking results.

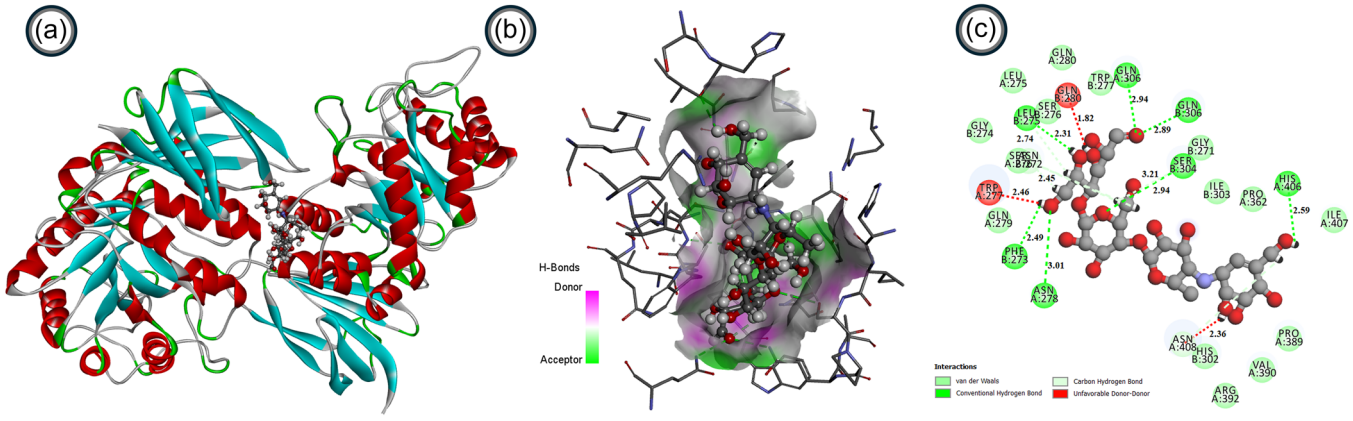
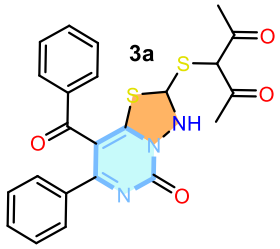


FIGURE 16 The position of the Acarbose ligand in the PDB: 1R47 protein (a), 3D (b), and 2D (c) molecular docking results.

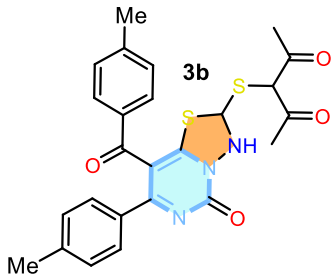
15214184, 0, Downloaded from https://onlinelibrary.wiley.com/doi/10.1002/ardp.202300634 by BOZOK UNIVERSITY-YOZGAT, Wiley Online Library on [21/05/2024]. See the Terms and Conditions (https://onlinelibrary.wiley.com/terms-and-conditions) on Wiley Online Library for rules of use; OA articles are governed by the applicable Creative Commons License

3-[(7-Benzoyl-6-phenyl-4-oxo-2,3-dihydro-4*H*-[1,3,4]thiadiazolo[3,2-*c*]pyrimidine-2-yl)thio]pentane-2,4-dione (3a):



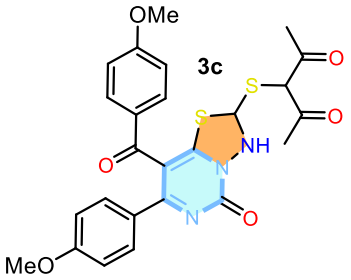
Yield: 56%, White crystalline solid (recrystallized from ethanol); M.P. = 193°C; FT-IR (ATR, cm^{-1}): 3298 (N–H), 3053 (arom. C–H), 2912 (aliph. C–H), 1703, 1637, 1614 (C=O), 1597, 1545, 1493 (C=C, C=N), 1178 (C-S); ^{1}H NMR (400 MHz, DMSO-d_6, δ, ppm): 10.32 (s, 1H, NH), 7.13–6.94 (m, 10H, Ar-H), 5.25 (s,1H, CH), 2.39 (s, 3H, CH_3), 2.16 (s, 3H, CH_3); ^{13}C NMR (100 MHz, DMSO-d_6, δ, ppm): 200.38, 199.21, 197.49, 195.21 (C=O), 151.33, 147.66, 140.01, 133.86, 130.63, 130.44, 130.16, 129.01, 128.16, 127.55, 104.02 (arom. C's), 74.12 (CH), 59.71 (S-CH-S), 29.69, 29.05 (2 × CH_3). Anal. Calcd. for $C_{23}H_{19}N_3O_4S_2$ (465,54 g/mol): C, 59.34; H, 4.11; N, 9.03; S, 13.78. Found: C, 59.12; H, 4.38; N, 9.42; S, 13.97.

3-{[7-(4-Methylbenzoyl)-6-(4-methylphenyl)-4-oxo-2,3-dihydro-4*H*-[1,3,4]thiadiazolo[3,2-*c*]pyrimidine-2-yl]thio}pentane-2,4-dione (3b)
:



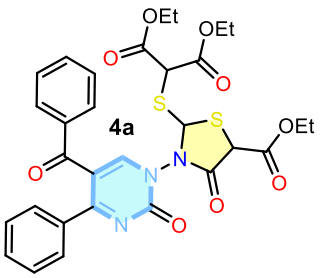
Yield: 77%, White crystalline solid (recrystallized from butanol); M.P. = 209°C; FT-IR (ATR, cm^{-1}): 3263 (N–H), 3036 (arom. C–H), 2999, 2912 (aliph. C–H), 1728, 1693, 1686, 1651 (C=O), 1589, 1562, 1510, 1471 (C=C, C=N), 1186 (C-S); ^{1}H NMR (400 MHz, DMSO-d_6, δ, ppm): 10.22 (s, 1H, NH), 7.75–6.77 (m, 8H, Ar-H), 5.20 (s,1H, CH), 2.26 (s, 3H, CH_3), 2.15 (s, 3H, CH_3), 2.11 (2 × s, 6H, 2 × CH_3); ^{13}C NMR (100 MHz, DMSO-d_6, δ, ppm): 200.38, 197.30, 194.92 (C=O), 147.78, 140.54, 140.37, 137.26, 130.52, 130.03, 129.28, 128.61, 128.09, 103.73 (arom. C's), 74.24 (CH), 59.84 (S-CH-S), 29.62, 29.07 (2 × CH_3), 21.26, 21.18 (2 × CH_3). Anal. Calcd. for $C_{25}H_{23}N_3O_4S_2$ (493,59 g/mol): C, 60.83; H, 4.70; N, 8.51; S, 12.99. Found: C, 61.22; H, 4.92; N, 8.86; S, 12.59.

3-{[7-(4-Methoxybenzoyl)-6-(4-methoxyphenyl)-4-oxo-2,3-dihydro-4*H*-[1,3,4]thiadiazolo[3,2-*c*]pyrimidine-2-yl]thio}pentane-2,4-dione (3c):



Yield: 86%, White crystalline solid (recrystallized from butanol); M.P. = 216°C; FT-IR (ATR, cm^{-1}): 3229 (N–H), 3036 (arom. C–H), 2964, 2843 (aliph. C–H), 1728, 1686, 1637 (C=O), 1607, 1589, 1576, 1501 (C=C, C=N), 1186 (C–S); ^{1}H NMR (400 MHz, DMSO-d_6, δ, ppm): 10.17 (s, 1H, NH), 7.15–6.53 (m, 8H, Ar–H), 5.17 (s, 1H, CH), 3.64, 3.62 (2 s, 6H, 2 × OCH_3), 2.35, 2.15 (s, 6H, 2 × CH_3); ^{13}C NMR (100 MHz, DMSO-d_6, δ, ppm): 197.17, 194.04, 162.34, 160.94 (C=O), 147.88, 132.31, 131.68, 131.28, 131.03, 125.68, 114.36, 114.22, 113.70, 113.04, 103.30 (arom. C's), 74.49 (CH_3), 60.08 (S–CH–S), 55.69, 55.65 (2 × CH_3O), 29.52, 29.12 (2 × CH_3). Anal. Calcd. for $C_{25}H_{23}N_3O_6S_2$ (525,29 g/mol): C, 57.13; H, 4.41; N, 7.99; S, 12.20. Found: C, 57.05; H, 4.19; N, 8.15; S, 12.00.

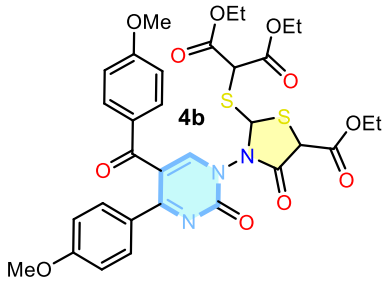
5-Benzoyl-4-phenyl-2-oxo-1(2*H*)-[4-ethylmethanoat-2-(diethylpropanoat-thio)-1,3-thiazol-5-one-1-yl]pyrimidine (4a)
:



Yield: 58%, White crystalline solid (recrystallized from butanol); M.P. = 130°C; FT-IR (ATR, cm^{-1}): 3105 (arom. C–H), 2964 (aliph. C–H), 1738, 1686 (C=O), 1614, 1580, 1413 (C=C, C=N), 1249 (C–S); ^{1}H NMR (400 MHz, $CDCl_3$, δ, ppm): 7.39–6.97 (m, 11H, Ar-H), 5.56 (s, 1H, CH), 5.32 (s, 1H, CH) 4.34–4.25 (m, 6H, 3 × CH_2), 1.36–1.27 (m, 9H, 3 × CH_3); ^{13}C NMR (100 MHz, $CDCl_3$, δ, ppm): 194.18, 165.95, 165.50, 165.15, 163.40 (C=O), 147.77, 147.42, 146.92, 138.66, 133.68, 131.10, 130.15, 129.35, 128.57, 128.41, 127.36, 105.71 (arom. C's), 63.75, 63.03, 62.90 (3 × OCH_2), 62.20, 60.12, 53.01 (3 × CH), 14.01-13.42 (3 × CH_3). Anal. Calcd. for $C_{30}H_{28}N_3O_9S_2$ (638.69 g/mol): C, 56.42; H, 4.42; N, 6.58; S, 10.04. Found: C, 56.78; H, 4.59; N, 6.96; S, 10.37.

15214184, 0, Downloaded from https://onlinelibrary.wiley.com/doi/10.1002/ardp.202300634 by BOZOK UNIVERSITY-YOZGAT, Wiley Online Library on [21/05/2024]. See the Terms and Conditions (https://onlinelibrary.wiley.com/terms-and-conditions) on Wiley Online Library for rules of use; OA articles are governed by the applicable Creative Commons License

5-(4-Methoxybenzoyl)-4-(4-methoxyphenyl)-2-oxo-1(2*H*)-[4-ethylmethanoat-2-(diethylpropanoat-thio)-1,3-thiazol-5-one-1-yl] pyrimidine (4b):



Yield: 62%, White crystalline solid (recrystallized from 2-propanol); M.P. = 149°C; FT-IR (ATR, cm^{-1}): 3140 (arom. C–H), 2982, 2843 (aliph. C–H), 1728, 1693 (C=O), 1583, 1510, 1458 (C=C, C=N), 1230 (C–S), 1178 (ester, C–O–C); ^1H NMR (400 MHz, $CDCl_3$, δ, ppm): 7.43–6.53 (m, 9H, Ar-H), 5.53 (s, 1H, CH), 5.31 (s, 1H, CH), 4.34–4.27 (m, 6H, 3 × OCH_2), 3.72, 3.69 (s, 6H, 2 × OCH_3), 1.36–1.27 (m, 9H, 3 × CH_3); ^{13}C NMR (100 MHz, $CDCl_3$, δ, ppm): 192.82, 165.93, 165.53, 165.17, 163.42 (C=O), 162.00, 160.78, 147.51, 144.91, 131.65, 129.85, 126.18, 113.92, 112.76, 105.38, 99.98 (arom. C's), 63.64, 63.01, 62.90 (3 × OCH_2), 62.39, 60.44 (2 × OCH_3), 55.30, 55.25, 53.13 (3 × CH), 14.01-13.43 (3 × CH_3). Anal. Calcd. for $C_{32}H_{32}N_3O_{11}S_2$ (699.75 g/mol): C, 54.93; H, 4.75; N, 6.01; S, 9.16. Found: C, 54.86; H, 4.59; N, 6.36; S, 9.01.

4.2 | Enzymes inhibition and reagents

4.2.1 | The activity of CAs

hCA I and II isoenzymes were purified using the Sepharose-4B-L-Tyrosine-sulfanilamide affinity technique.[72,73] Then, the purity of these CA isoenzymes was defined via the SDS-PAGE purity technique.[74] The inhibition effects of compounds versus the esterase activity of the hCAs were determined by following the change in absorbance at 348 nm according to the assay defined by Verpoorte methods[72,75] as described previously.[76,77] The quantity of protein was spectrophotometrically recorded at 595 nm according to Bradford's method[78] as detailed in a previous study.[79] The hCA activities were measured using 4-nitrophenyl acetate as in a previous study.[80] All the measurements were repeated thrice.

4.2.2 | The activity of anticholinesterase

AChE and BChE activities were assessed using a modified version of the Ellman method[81] as detailed in a prior study.[79] The measurement of AChE/BChE activity was conducted with acetylthiocholine iodide and butyrylcholine iodate as substrates, along with 5,5-dithiobis(2-nitrobenzoic) acid. Substrate utilization was monitored spectrophotometrically at 412 nm.[82]

4.2.3 | α-Glycosidase activity

The inhibitory effect of novel compounds (**2a–c**, **3a–c**, **4a,b**) on α-glycosidase was investigated using *p*-nitrophenyl-D-glycopyranoside as the substrate,[83] following the procedures outlined in a previous study.[84] Absorbance values were measured spectrophotometrically at 405 nm.[84]

4.2.4 | The activity of AR

The measurement of AR activity involved monitoring the decrease in absorbance of NADPH at 340 nm using a spectrophotometer.[85] The enzymatic reaction mixture, with a total volume of approximately 1 mL, was composed of 0.1 M sodium phosphate buffer (pH: 5.5), 4.7 mM DL-glyceraldehyde, 0.11 mM NADPH, and the enzyme solution.[86,87]

4.2.5 | In vitro inhibition studies

The inhibitory effects of the newly synthesized compounds were assessed using a minimum of five different inhibitor concentrations for hCAs, AChE, BChE, AR, and α-glycosidase. The IC_{50} values for these synthesized derivatives were determined from the graphs of Activity (%) versus [Synthesized derivatives] for each compound.[88] Inhibition types and K_i values were determined using Lineweaver and Burk's curves.[89]

4.3 | Computational details

The in silico docking studies were carried out using the AutoDock Vina tool.[55] Optimization of the molecules was performed for the ground state and gas phase using the Gaussian 09 W package program[56] with the DFT/B3LYP (theory/functional) and the 6-311++G(d,p) basis set. In addition, three-dimensional views of the structures were created with the help of Gauss View program[57] without any symmetrical constraints.

ACKNOWLEDGMENTS

The authors would like to thank the Scientific Research Projects Coordination Unit Coordinatorship of Erciyes University for financial support (Project no: FBA-2013-4215). The synthesis and characterization of the compounds presented in this article are part of the master's thesis work of Seher Arslan and Hava Aydın.

CONFLICT OF INTEREST STATEMENT

The authors declare no conflicts of interest.

DATA AVAILABILITY STATEMENT

Data are available on request from the authors.

15214184, 0, Downloaded from https://onlinelibrary.wiley.com/doi/10.1002/ardp.202300634 by BOZOK UNIVERSITY-YOZGAT, Wiley Online Library on [21/05/2024]. See the Terms and Conditions (https://onlinelibrary.wiley.com/terms-and-conditions) on Wiley Online Library for rules of use; OA articles are governed by the applicable Creative Commons License

ORCID

Elif Korkusuz http://orcid.org/0000-0001-6375-8140
Yusuf Sert http://orcid.org/0000-0001-8836-8667
İsmail Yıldırım http://orcid.org/0000-0001-7986-3236
Yeliz Demir http://orcid.org/0000-0003-3216-1098
İlhami Gülçin http://orcid.org/0000-0001-5993-1668
İrfan Koca http://orcid.org/0000-0001-7873-159X

REFERENCES

[1] D. F. Smee, P. A. McKernan, L. D. Nord, R. C. Willis, C. R. Petrie, T. M. Riley, G. R. Revankar, R. K. Robins, R. A. Smith, *Antimicrob. Agents Chemother.* **1987**, *31*, 1535.
[2] K. Umesha, B. K. Sarojini, C. G. Darshan Raj, V. Bhanuprakash, R. Yogisharadhya, R. Raghavendra, M. T. H. Khan, *Med. Chem. Res.* **2014**, *23*, 168.
[3] H. S. Khalaf, H. Tolan, M. Radwan, A. M. Mohamed, H. M. Awad, W. A. El-Sayed, *Nucleosides Nucleotides Nucleic Acids* **2020**, *39*, 1036.
[4] D. Dheer, V. Singh, R. Shankar, *Bioorg. Chem.* **2017**, *71*, 30.
[5] N. A. Abdel-Latif, N. M. Sabry, A. M. Mohamed, M. M. Abdulla, *Monatsh. Chem.-Chem. Monthly* **2007**, *138*, 715.
[6] A. G. Amr, A. M. Mohamed, S. F. Mohamed, N. A. Abdel-Hafez, A. Hammam, *Bioorg. Med. Chem.* **2006**, *14*, 5481.
[7] S. Balalaie, M. Bararjanian, F. Rominger, *J. Heterocycl. Chem.* **2006**, *43*, 821.
[8] V. J. Ram, A. Goel, M. Nath, P. Srivastava, *Bioorg. Med. Chem. Lett.* **1994**, *4*, 2653.
[9] S. F. Mohamed, E. M. Flefel, A. E.-G. E. Amr, D. N. Abd El-Shafy, *Eur. J. Med. Chem.* **2010**, *45*, 1494.
[10] D. Cai, Z.-H. Zhang, Y. Chen, X.-J. Yan, S.-T. Zhang, L.-J. Zou, L.-H. Meng, F. Li, B.-J. Fu, *Med. Chem. Res.* **2016**, *25*, 292.
[11] A. M. Alqahtani, *Sci. Rep.* **2021**, *11*, 15750.
[12] K. Matsuno, Y. Masuda, Y. Uehara, H. Sato, A. Muroya, O. Takahashi, T. Yokotagawa, T. Furuya, T. Okawara, M. Otsuka, N. Ogo, T. Ashizawa, C. Oshita, S. Tai, H. Ishii, Y. Akiyama, A. Asai, *ACS Med. Chem. Lett.* **2010**, *1*, 371.
[13] B. H. Lee, M. F. Clothier, F. E. Dutton, G. A. Conder, S. S. Johnson, *Bioorg. Med. Chem. Lett.* **1998**, *8*, 3317.
[14] R. A. Coburn, R. A. Glennon, Z. F. Chmielewicz, *J. Med. Chem.* **1974**, *17*, 1025.
[15] B. Clare, *Eur. J. Med. Chem.* **2000**, *35*, 859.
[16] K. R. Sathisha, S. A. Khanum, J. N. Chandra, F. Ayisha, S. Balaji, G. K. Marathe, S. Gopal, K. S. Rangappa, *Bioorg. Med. Chem.* **2011**, *19*, 211.
[17] F. Alizadeh-Bami, H. Mehrabi, *Polycyclic Aromat. Compd.* **2023**, *43*, 7343.
[18] F. Özbey, P. Taslimi, İ. Gülçin, A. Maraş, S. Göksu, C. T. Supuran, *J. Enzyme Inhib. Med. Chem.* **2016**, *31*, 79.
[19] K. Kucukoglu, H. I. Gul, P. Taslimi, I. Gulcin, C. T. Supuran, *Bioorg. Chem.* **2019**, *86*, 316.
[20] Ö. Güleç, C. Türkeş, M. Arslan, Y. Demir, Y. Yeni, A. Hacımüftüoğlu, E. Ereminsoy, Ö. İ. Küfrevioğlu, Ş. Beydemir, *Mol. Divers.* **2022**, *26*, 2825.
[21] S. Göksu, A. Naderi, Y. Akbaba, P. Kalın, A. Akıncıoğlu, I. Gülçin, S. Durdagi, R. E. Salmas, *Bioorg. Chem.* **2014**, *56*, 75.
[22] C. Yamali, H. I. Gul, T. Cakir, Y. Demir, I. Gulcin, *Lett. Drug Des. Discov.* **2020**, *17*, 1283.
[23] M. Tugrak, H. I. Gul, Y. Demir, S. Levent, I. Gulcin, *Arch. Pharm. (Weinheim)* **2021**, *354*, 2000375.
[24] Y. Kaya, A. Erçağ, Y. Zorlu, Y. Demir, İ. Gülçin, *J. Biol. Inorg. Chem.* **2022**, *27*, 271.
[25] S. Bilginer, H. I. Gul, B. Anil, Y. Demir, I. Gulcin, *Arch. Pharm. (Weinheim)* **2021**, *354*, 2000243.
[26] B. O. Aydin, D. Anil, Y. Demir, *Arch. Pharm. (Weinheim)* **2021**, *354*, 2000330.
[27] M. Tugrak, H. I. Gul, Y. Demir, I. Gulcin, *Arch. Pharm. (Weinheim)* **2021**, *354*, 2000230.
[28] C. Kakakhan, C. Türkeş, Ö. Güleç, Y. Demir, M. Arslan, G. Özkemahlı, Ş. Beydemir, *Bioorg. Med. Chem.* **2023**, *77*, 117111.
[29] A. Aktaş, G. Yakalı, Y. Demir, İ. Gülçin, M. Aygün, Y. Gök, *Heliyon* **2022**, *8*, e10625.
[30] E. R. Buabeng, M. Henary, *Bioorg. Med. Chem.* **2021**, *39*, 116140.
[31] N. Oztaskin, S. Goksu, Y. Demir, A. Maras, İ. Gulcin, *Molecules* **2022**, *27*, 7426.
[32] R. Zengin, Y. Gök, Y. Demir, B. Şen, T. Taskin-Tok, A. Aktaş, Ö. Demirci, İ. Gülçin, M. Aygün, *J. Fluorine Chem.* **2023**, *267*, 110094.
[33] N. Öztaskın, P. Taslimi, A. Maraş, İ. Gülcin, S. Göksu, *Bioorg. Chem.* **2017**, *74*, 104.
[34] E. Bursal, A. Aras, Ö. Kılıç, P. Taslimi, A. C. Gören, İ. Gülçin, *J. Food Biochem.* **2019**, *43*, 12776.
[35] S. Burmaoglu, A. O. Yilmaz, M. F. Polat, R. Kaya, İ. Gulcin, O. Algul, *Bioorg. Chem.* **2019**, *85*, 191.
[36] S. Mitra, M. Muni, N. J. Shawon, R. Das, T. B. Emran, R. Sharma, D. Chandran, F. Islam, M. J. Hossain, S. Z. Safi, *Oxid.Med. Cell. Longev.* **2022**, *2022*, 7252882.
[37] F. S. Tokalı, Y. Demir, İ. H. Demircioğlu, C. Türkeş, E. Kalay, K. Şendil, Ş. Beydemir, *Drug Dev. Res.* **2022**, *83*, 586.
[38] M. I. Abdjan, N. S. Aminah, A. N. Kristanti, I. Siswanto, B. Ilham, A. P. Wardana, Y. Takaya, *RSC Adv.* **2023**, *13*, 3438.
[39] İ. Gülçin, B. Trofimov, R. Kaya, P. Taslimi, L. Sobenina, E. Schmidt, O. Petrova, S. Malysheva, N. Gusarova, V. Farzaliyev, A. Sujayev, S. Alwasel, C. T. Supuran, *Bioorg. Chem.* **2020**, *103*, 104171.
[40] İ. Gulçin, P. Taslimi, A. Aygün, N. Sadeghian, E. Bastem, O. I. Kufrevioglu, F. Turkan, F. Şen, *Int. J. Biol. Macromol.* **2018**, *119*, 741.
[41] P. Taslimi, H. E. Aslan, Y. Demir, N. Oztaskin, A. Maraş, İ. Gulçin, S. Beydemir, S. Goksu, *Int. J. Biol. Macromol.* **2018**, *119*, 857.
[42] N. Lolak, S. Akocak, C. Türkeş, P. Taslimi, M. Işık, Ş. Beydemir, İ. Gülçin, M. Durgun, *Bioorg. Chem.* **2020**, *100*, 103897.
[43] B. Sever, M. D. Altıntop, Y. Demir, M. Pekdoğan, G. Akalın Çiftçi, Ş. Beydemir, A. Özdemir, *J. Mol. Struct.* **2021**, *1224*, 129446.
[44] B. Sever, M. D. Altıntop, Y. Demir, N. Yılmaz, G. Akalın Çiftçi, Ş. Beydemir, A. Özdemir, *Chem. Biol. Interact.* **2021**, *345*, 109576.
[45] M. Akdağ, A. B. Özçelik, Y. Demir, Ş. Beydemir, *J. Mol. Struct.* **2022**, *1258*, 132675.
[46] M. A. Ramirez, N. L. Borja, *Pharmacother. J. Hum. Pharmacol. Drug Ther.* **2008**, *28*, 646.
[47] F. Panahi, R. Yousefi, M. H. Mehraban, A. Khalafi-Nezhad, *Carbohydr. Res.* **2013**, *380*, 81.
[48] F. Balestri, L. Quattrini, V. Coviello, S. Sartini, F. Da Settimo, M. Cappiello, R. Moschini, A. Del Corso, U. Mura, C. La Motta, *Cell Chem. Biol.* **2018**, *25*, 1414.
[49] C. La Motta, S. Sartini, L. Mugnaini, F. Simorini, S. Taliani, S. Salerno, A. M. Marini, F. Da Settimo, A. Lavecchia, E. Novellino, M. Cantore, P. Failli, M. Ciuffi, *J. Med. Chem.* **2007**, *50*, 4917.
[50] M. Bortolami, F. Pandolfi, V. Tudino, A. Messore, V. N. Madia, D. De Vita, R. Di Santo, R. Costi, I. Romeo, S. Alcaro, M. Colone, A. Stringaro, A. Espargaró, R. Sabatè, L. Scipione, *ACS Chem. Neurosci.* **2021**, *12*, 4090.
[51] B. Kumar, A. R. Dwivedi, B. Sarkar, S. K. Gupta, S. Krishnamurthy, A. K. Mantha, J. Parkash, V. Kumar, *ACS Chem. Neurosci.* **2018**, *10*, 252.
[52] B. Altural, G. Kollenz, *Monatsh. Chem. Chem. Monthly* **1990**, *121*, 677.
[53] Z. ÖNAL, B. Altural, *Turk. J. Chem.* **1999**, *23*, 401.
[54] İ. Yildirim, I. Koca, *Kuwait J. Sci. Eng.* **2005**, *32*, 49.
[55] O. Trott, A. J. Olson, *J. Comput. Chem.* **2010**, *31*, 455.

15214184, 0, Downloaded from https://onlinelibrary.wiley.com/doi/10.1002/ardp.202300634 by BOZOK UNIVERSITY-YOZGAT, Wiley Online Library on [21/05/2024]. See the Terms and Conditions (https://onlinelibrary.wiley.com/terms-and-conditions) on Wiley Online Library for rules of use; OA articles are governed by the applicable Creative Commons License

[56] M. Frisch, G. Trucks, H. Schlegel, G. Scuseria, M. Robb, J. Cheeseman, G. Scalmani, V. Barone, B. Mennucci, G. Petersson, *Gaussian 09*, *Revision D. 01*, Gaussian, Inc., Wallingford CT **2009**.
[57] R. Dennington, T. Keith, J. Millam, *GaussView*, *Version 5*, Semichem Inc., Shawnee Mission, KS **2009**.
[58] L. Ferreira, R. Dos Santos, G. Oliva, A. Andricopulo, *Molecules* **2015**, *20*, 13384.
[59] http://www.3dsbiovia.com/
[60] K. K. Kannan, M. Ramanadham, T. A. Jones, *Ann. N. Y. Acad. Sci.* **1984**, *429*, 49.
[61] I. Mahmudov, Y. Demir, Y. Sert, Y. Abdullayev, A. Sujayev, S. H. Alwasel, I. Gulcin, *Arabian J. Chem.* **2022**, *15*, 103645.
[62] J. Ivanova, J. Leitans, M. Tanc, A. Kazaks, R. Zalubovskis, C. T. Supuran, K. Tars, *Chem. Commun.* **2015**, *51*, 7108.
[63] G. Kryger, I. Silman, J. L. Sussman, *Structure* **1999**, *7*, 297.
[64] U. Košak, B. Brus, D. Knez, S. Žakelj, J. Trontelj, A. Pišlar, R. Šink, M. Jukič, M. Živin, A. Podkowa, F. Nachon, X. Brazzolotto, J. Stojan, J. Kos, N. Coquelle, K. Sałat, J. P. Colletier, S. Gobec, *J. Med. Chem.* **2018**, *61*, 119.
[65] P. Taslimi, F. Akhundova, M. Kurbanova, F. Türkan, B. Tuzun, A. Sujayev, N. Sadeghian, A. Maharramov, V. Farzaliyev, İ. Gülçin, *Polycyclic Aromat. Compd.* **2021**, 1.
[66] S. C. Garman, D. N. Garboczi, *J. Mol. Biol.* **2004**, *337*, 319.
[67] X. Zheng, L. Zhang, W. Chen, Y. Chen, W. Xie, X. Hu, *ChemMedChem* **2012**, *7*, 1921.
[68] Y. Demir, P. Taslimi, Ü. M. Koçyiğit, M. Akkuş, M. S. Özaslan, H. E. Duran, Y. Budak, B. Tüzün, M. B. Gürdere, M. Ceylan, S. Taysi, İ. Gülçin, Ş. Beydemir, *Arch. Pharm. (Weinheim)* **2020**, *353*, 2000118.
[69] https://www.rcsb.org/
[70] K. Farzam, M. Abdullah, *Acetazolamide*, *StatPearls [Internet]*, StatPearls Publishing, Treasure Island (FL) **2024**. https://www.ncbi.nlm.nih.gov/books/NBK532282/
[71] S. A. Eagger, R. Levy, B. J. Sahakian, *Lancet* **1991**, *337*, 989.
[72] J. A. Verpoorte, S. Mehta, J. T. Edsall, *J. Biol. Chem.* **1967**, *242*, 4221.
[73] Y. Akbaba, A. Akıncıoğlu, H. Göçer, S. Göksu, İ. Gülçin, C. T. Supuran, *J. Enzyme Inhib. Med. Chem.* **2014**, *29*, 35.
[74] P. Taslimi, İ. Gülçin, N. Öztaşkın, Y. Çetinkaya, S. Göksu, S. H. Alwasel, C. T. Supuran, *J. Enzyme Inhib. Med. Chem.* **2016**, *31*, 603.
[75] T. Coban, S. Beydemir, I. Gülçin, D. Ekinci, *J. Enzyme Inhib. Med. Chem.* **2008**, *23*, 266.
[76] M. Güney, A. Coşkun, F. Topal, A. Daştan, İ. Gülçin, C. T. Supuran, *Bioorg. Med. Chem.* **2014**, *22*, 3537.
[77] O. Hisar, Ş. Beydemir, İ. Gülçin, Ö. İ. Küfrevioğlu, C. T. Supuran, *J. Enzyme Inhib. Med. Chem.* **2005**, *20*, 35.
[78] M. M. Bradford, *Anal. Biochem.* **1976**, *72*, 248.
[79] P. Taslimi, H. Akıncıoglu, İ. Gülçin, *J. Biochem. Mol. Toxicol.* **2017**, *31*, e21973.
[80] D. Ozmen Ozgun, H. I. Gul, C. Yamali, H. Sakagami, I. Gulcin, M. Sukuroglu, C. T. Supuran, *Bioorg. Chem.* **2019**, *84*, 511.
[81] G. L. Ellman, K. D. Courtney, V. Andres Jr., R. M. Featherstone, *Biochem. Pharmacol.* **1961**, *7*, 88.
[82] E. Palabıyık, A. N. Sulumer, H. Uguz, B. Avcı, S. Askın, H. Askın, Y. Demir, *J. Mol. Recognit.* **2023**, *36*, e3004.
[83] Y. Tao, Y. Zhang, Y. Cheng, Y. Wang, *Biomed. Chromatogr.* **2013**, *27*, 148.
[84] P. Taslimi, F. M. Kandemir, Y. Demir, M. İleritürk, Y. Temel, C. Caglayan, İ. Gulçin, *J. Biochem. Mol. Toxicol.* **2019**, *33*, e22313.
[85] M. J. Cerelli, D. L. Curtis, J. P. Dunn, P. H. Nelson, T. M. Peak, L. D. Waterbury, *J. Med. Chem.* **1986**, *29*, 2347.
[86] N. Abul, S. Gerni, I. N. Korkmaz, Y. Demir, H. Özdemir, İ. Gülçin, *Chem. Biodivers.* **2023**, *20*, 202300687.
[87] H. Çelik Onar, E. M. Özden, H. D. Taslak, İ. Gülçin, A. Ece, E. Erçağ, *Chem. Biol. Interact.* **2023**, *383*, 110655.
[88] İ. Gulcin, S. H. Alwasel, *Processes* **2022**, *10*, 132.
[89] H. Lineweaver, D. Burk, *J. Am. Chem. Soc.* **1934**, *56*, 658.

SUPPORTING INFORMATION

Additional supporting information can be found online in the Supporting Information section at the end of this article.

How to cite this article: E. Korkusuz, Y. Sert, S. Arslan, H. Aydın, İ. Yıldırım, Y. Demir, İ. Gülçin, İ. Koca, *Arch. Pharm.* **2024**, e2300634. https://doi.org/10.1002/ardp.202300634

15214184, 0, Downloaded from https://onlinelibrary.wiley.com/doi/10.1002/ardp.202300634 by BOZOK UNIVERSITY-YOZGAT, Wiley Online Library on [21/05/2024]. See the Terms and Conditions (https://onlinelibrary.wiley.com/terms-and-conditions) on Wiley Online Library for rules of use; OA articles are governed by the applicable Creative Commons License